International Journal of Climatology

RMetS Royal Meteorological Society

Long-term variability and trends in meteorological droughts in Western Europe (1851-2018)

Journal:	*International Journal of Climatology*
Manuscript ID	JOC-19-0988.R2
Wiley - Manuscript type:	Research Article
Date Submitted by the Author:	12-Jun-2020
Complete List of Authors:	Vicente-Serrano, Sergio; Consejo Superior de Investigaciones Cientificas, Instituto Pirenaico de Ecología; Domínguez-Castro, Fernando; Universidad de Zaragoza, Geografía Murphy, Conor; Maynooth University, Irish Climate Analysis and Research UnitS (ICARUS), Department of Geography Hannaford, Jamie; CEH Wallingford, Water Resources Reig, Fergus; CSIC, Instituto Pirenaico de Ecología Peña-Angulo, Dhais; Consejo Superior de Investigaciones Cientificas, Instituto Pirenaico de Ecología Tramblay , Yves; IRD, HydroSciences Montpellier Trigo, Ricardo Trigo; Universidade de Lisboa Instituto Geofísico do Infante Dom Luiz, Faculdade de Ciências Macdonald, Neil; University of Liverpool, Geography Luna, Yolanda; State Meteorological Agency (Agencia Estatal de Meteorología/AEMET, AEMET McCarthy, Mark; Met Office, Hadley Centre van der Schrier, Gerard; Royal Netherlands Meteorol Inst KNMI, ---- Turco, Marco; University of Murcia, Physics Camuffo, Dario; Institute of Atmospheric Sciences and Climate of the National Research Council (ISAC-CNR), --- Noguera, Ivan; CSIC, Instituto Pirenaico de Ecología García-Herrera, Ricardo; Universidade Complutense, Facultad de Físicas, Departamento de Física da Terra II Becherini, Francesca; Institute of Atmospheric Sciences and Climate of the National Research Council (ISAC-CNR), --- Della Valle, Antonio; Institute of Atmospheric Sciences and Climate of the National Research Council (ISAC-CNR), --- Tomas-Burguera, Miquel; Estación Experimental de Aula Dei (EEAD-CSIC), Suelo y agua El Kenawy, Ahmed; Mansoura University, Geography
Keywords:	Observations < 1. Tools and methods, Rainfall < 3. Physical phenomenon, Climate < 6. Application/context
Country Keywords:	Austria, Belgium, Croatia, Czech Republic, France

Long-term variability and trends in meteorological droughts in Western Europe (1851-2018)

Vicente-Serrano, S.M.[1], Domínguez-Castro, F.[2], Murphy, C.[3], Hannaford, J.[3,4], Reig, F.[1], Peña-Angulo, D.[1], Tramblay, Y.[5], Trigo, R.M.[6], MacDonald, N.[7], Luna, M.Y.[8], McCarthy, M.[9], Van der Schrier, G.[10], Turco, M.[11], Camuffo, D.[12], Noguera, I.[1], García-Herrera, R.[13,14], Becherini, F.[12,15], della Valle, A.[12], Tomas-Burguera, M.[16], El Kenawy, A.[17,18]

[1]Instituto Pirenaico de Ecología, Consejo Superior de Investigaciones Científicas (IPE–CSIC), Zaragoza, Spain,

[2]Aragonese Agency for Research and Development Researcher, Department of Geography, University of Zaragoza, Zaragoza, Spain

[3]Irish Climate Analysis and Research UnitS (ICARUS), Department of Geography, Maynooth University, Maynooth, Ireland,

[4]Centre for Ecology and Hydrology, Wallingford, United Kingdom,

[5]HSM (Univ. Montpellier, CNRS, IRD), Montpellier, France

[6]Instituto Dom Luiz (IDL), Faculdade de Ciências, Universidade de Lisboa, Lisboa, Portugal

[7]School of Environmental Sciences, University of Liverpool, Liverpool

[8]Agencia Estatal de Meteorología (AEMET), Madrid, Spain

[9]Met Office National Climate Information Centre, Exeter, United Kingdom,

[10]Royal Netherlands Meteorological Institute (KNMI), De Bilt, Netherlands

[11]Regional Atmospheric Modeling Group, Department of Physics, University of Murcia, Spain

[12]Institute of Atmospheric Sciences and Climate (CNR-ISAC), Padova, Italy

[13] Departamento de Ciencias de la Tierra y Astrofísica, Facultad de Ciencias Físicas, Universidad Complutense de Madrid, Madrid, Spain

[14] Instituto de Geociencias (CIS-UCM) Madrid, Spain

[15] Institute of Polar Sciences (CNR-ISP), Venice, Italy

[16]Estación Experimental de Aula Dei, Consejo Superior de Investigaciones Científicas (EEAD–CSIC), Zaragoza, Spain.

[17]Department of Geography, Mansoura University, Mansoura, Egypt

[18]Department of Geography, Sultan Qaboos University, Al Khoud, Muscat, Oman

Abstract: We analyzed long-term variability and trends in meteorological droughts across Western Europe using the Standardized Precipitation Index (SPI). Precipitation data from 199 stations spanning the period 1851-2018 were employed, following homogenisation, to derive SPI-3 and SPI-12 series for each station, together with indices on drought duration and severity. Results reveal a general absence of statistically significant long-term trends in the study domain, with the exception of significant trends at some stations, generally covering short periods. The largest decreasing trends in SPI-3 (i.e. increasing drought conditions) were found for summer in the British and Irish Isles. In general, drought episodes experienced in the last two or three decades have precedents during the last 170 years, emphasising the importance of long records for assessing change. The main characteristic of drought variability in Western Europe is its strong spatial diversity, with regions exhibiting a homogeneous temporal evolution. Notably, the temporal variability of drought in Western Europe is more dominant than long-term trends. This suggests that long-term drought trends cannot be confirmed in Western Europe using precipitation records alone. This study provides a long-term regional assessment of drought variability in Western Europe, which can contribute to better understanding of regional climate change during the past two centuries.

Keywords: Standardized Precipitation Index; Drought; Precipitation; Instrumental Period; Trends; Western Europe; Mediterranean.

1. Introduction

Many studies have analyzed droughts across Europe (e.g. Bordi *et al.*, 2009; Brázdil *et al.*, 2015; Potop *et al.*, 2014; Todd *et al.*, 2013; van der Schrier *et al.*, 2006). Drying trends have been suggested over the Mediterranean region (e.g. Hoerling *et al.*, 2012; Sousa *et al.*, 2011; Stagge *et al.*, 2017; Vicente-Serrano *et al.*, 2014c), particularly due to anthropogenic influences (Gudmundsson *et al.*, 2017; Gudmundsson and Seneviratne, 2016; Hoerling *et al.*, 2012). These trends have been supported by several

studies based on paleo-climatic reconstructions and modelling approaches (e.g. Briffa *et al.*, 2009; Hanel *et al.*, 2018; Marvel *et al.*, 2019; Nicault *et al.*, 2008). However, other investigations that have employed precipitation-based drought indices have not found significant trends across Europe (e.g. Lloyd-Hughes and Saunders, 2002; Spinoni *et al.*, 2017, 2019), including the Mediterranean (e.g. Di Lena *et al.*, 2014; Domínguez-Castro *et al.*, 2019; Martins *et al.*, 2012; Merino *et al.*, 2015). The findings of these studies stress the difficulty in finding consensus on drought trends given the complexity of defining (Lloyd-Hughes, 2014) and quantifying (Vicente-Serrano, 2016; Wilhite and Pulwarty, 2017) drought. Furthermore, uncertainty in drought trends in Europe is linked to the use of different periods of analysis (Hannaford *et al.*, 2013) and deployment of a wide spectrum of possible drought metrics. The latter employ several hydroclimatic variables including, precipitation (Lloyd-Hughes and Saunders, 2002; Vicente-Serrano, 2006a), atmospheric evaporative demand (Spinoni *et al.*, 2015; Stagge *et al.*, 2017; Vicente-Serrano *et al.*, 2014b), streamflow (Hannaford *et al.*, 2013; Hisdal *et al.*, 2001; Lorenzo-Lacruz *et al.*, 2013; Parry *et al.*, 2012), groundwater (Lorenzo-Lacruz *et al.*, 2017; Marchant and Bloomfield, 2018) and soil moisture simulations (Hanel *et al.*, 2018; Moravec *et al.*, 2019).

In this context, the observed increase in atmospheric evaporative demand (AED), as revealed by Robinson *et al.* (2017), Stagge *et al.* (2017) and Vicente-Serrano *et al.* (2014a) could be seen as a key driver of drought severity in Europe over recent decades, particularly in the Mediterranean region (García-Herrera *et al.*, 2019; Stagge *et al.*, 2017; Vicente-Serrano *et al.*, 2014b). This may explain the decrease of soil moisture in land-atmosphere model outputs (e.g. Hanel *et al.*, 2018). Despite the significant role of AED, precipitation remains the dominant climatic variable contributing to recent drought severity and variability (Briffa *et al.*, 2009; Lloyd-Hughes and Saunders, 2002). This dependency is valid from a hydroclimatic perspective, given the stronger response of streamflow to precipitation, compared to AED (Yang *et al.*, 2018), which has been empirically verified for Western Europe (see Vicente-Serrano, *et al.*, 2019).

Future climate projections, based on different drought metrics, suggest that vast areas of Europe are likely to be impacted by severe drought events by the end of the 21st Century in response to anthropogenic forcing (e.g. Beniston *et al.*, 2007; Forzieri *et al.*, 2014; Samaniego *et al.*, 2018; Sheffield and Wood, 2008; Spinoni *et al.*, 2018). These events could be seen as an extension of observed drought episodes in Europe over the past two decades, including, for example: the 2011/2012 (Trigo *et al.*, 2013) and

2004/2005 (García-Herrera *et al.*, 2007; Santos *et al.*, 2007) droughts in Iberia, the 2003/2004 (Mihajlović, 2006) and 2012 (Cindrić *et al.*, 2016) in Croatia, the 2011/2012 (Zahradníček *et al.*, 2015) drought in the Czech Republic, the 2015 drought (Hoy *et al.*, 2017; Ionita *et al.*, 2017; Laaha *et al.*, 2017) in central Europe, and the 2017 drought (García-Herrera *et al.*, 2019) in Western Europe. However, a considerable number of intense drought events took place in Europe in the first half of the 20th century, but have not received a similar level of attention as those mentioned above (e.g. the 1944-45 Iberian drought or the widespread 1921-22 European drought). In fact, a long-term assessment of drought variability and changes in Western Europe remains lacking. Such an assessment is necessary to test whether present drought characteristics are unusual in the context of available instrumental observations.

Therefore, the main objectives of this study are: i) to analyse long-term (1851-2018) variability and trends in meteorological droughts over Western Europe, ii) to define the spatial patterns of these trends, and iii) to determine changes in the duration, magnitude and spatial extent of droughts. To realise these objectives we assess drought characteristics using the standardized precipitation index (SPI) applied to a newly developed precipitation dataset (199 long-term stations) covering Western Europe.

2. Data

Precipitation data were collected from different sources, including national meteorological agencies in different countries (e.g. Spain, Portugal, Germany, Netherlands, France, and the United Kingdom), the Global Historical Climatology Network (GHCN) dataset (https://www.ncdc.noaa.gov/data-access/land-based-station-data/land-based-datasets/global-historical-climatology-network-ghcn), the European Climate Assessment & Dataset (ECA&D) project (https://www.ecad.eu//dailydata/index.php), in addition to a set of long-term precipitation series presented in earlier works by Murphy *et al.* (2019), Noone *et al.* 2017 and Todd *et al.* (2015). Overall, we collected monthly precipitation data from 1871 locations across Western Europe covering the period from 1851 to 2018. Amongst them, data from only 206 observatories were retained, as they have short gaps (less than 5% of the total record missing).

The selected time series were subjected to rigorous quality control and homogeneity testing. The quality control was mainly based on a comparison of the anomaly of

precipitation at each candidate station with the closest five neighbouring stations. Herein, the anomalies were computed with respect to the base period 1871-2018 and compared for each month independently. This statistical testing was also supported by a careful visual assessment to compare data from each station with the closest reference stations. The aim was to trim suspicious values, while keeping 'real' extreme values. This procedure is important, given that some parts of the Mediterranean can experience exceptional local wet events during summertime. Following this procedure, data for 798 months (0.2% of the total dataset) were removed and assigned as "missing values". At the station level, the number of trimmed values was generally less than 5 data points over the whole study period (1851-2018) (Figure 1a).

To perform homogeneity testing, HOMER (HOMogenization software in R) was employed. HOMER is a semi-automated tool in the R platform, which combines a fully automated joint segmentation with a partly subjective pairwise comparison. This tool allows for identification of breaks in monthly precipitation series by means of a wide range of relative homogeneity tests. These tests are highly recommended for testing homogeneity of climate data (Venema *et al.*, 2012). According to the relative homogeneity tests, data from each candidate series were compared with data from a number of reference series (the best 5 correlated series) at both seasonal and annual scales (Mestre *et al.*, 2013; Noone *et al.*, 2016). When a statistically significant break is detected in a series, a correction factor was applied following Mestre *et al.* (2013). Figure 1b illustrates the frequency of inhomogeneities found in the dataset. As depicted, most of the series (*N=138*) were free from the presence of inhomogeneities, while the frequency of stations with two or more breaks was low. The dataset did not show a particular concentration of inhomogeneities over specific periods, which gives confidence in the overall high quality of the data (Figure 1c). Following homogeneity testing, only three stations were discarded due to the presence of a high number of inhomogeneities in the data and their weak correlation with neighbouring reference series. Figure 2 illustrates the spatial distribution of the final dataset following the results of the quality control and homogeneity testing. According to the data availability, the final dataset includes 115, 171 and 199 stations whose records date back to 1851, 1861 and 1871, respectively. It should be noted that the few missing values present in the series, due to quality control checks, were filled by HOMER after the homogeneity testing following the procedure detailed by Mestre *et al.* (2013).

3. Methods

The SPI is a standardized drought index that allows direct comparison over space and time, irrespective of precipitation magnitude and climatic conditions. Originally proposed by Mckee *et al.* (1993), SPI is one of the most widely-used drought metrics and is also recommended for drought monitoring by the WMO (Hayes *et al.*, 2011; WMO, 2012). To quantify drought, we computed SPI at two timescales (3- and 12-month) using precipitation data from 199 stations. 3-month allows identifying seasonal dryness and 12-month to determine the annual conditions. To ensure comparability of SPI series derived for different lengths (1851-2018, 1861-2018 and 1871-2018) the reference period used to calculate the distribution parameters in fitting SPI was 1871-2018 for all stations. SPI was derived using the SPEI package within the R platform (Beguería *et al.*, 2014) using the Gamma distribution following the guidelines of the World Meteorological Organization (WMO).

Drought characteristics were defined for each precipitation series in the study domain using the calculated SPI series. A drought event was simply defined using an SPI threshold comparable over space and time (Tallaksen *et al.*, 1997; 2009). A value equal to -0.84 represents the 20th percentile of the SPI cumulative probability distribution and return period of one in five years, thus ensuring a sufficient sample size for reliable trend detection. Drought duration was defined as the number of consecutive and uninterrupted months with SPI below -0.84, while the accumulated precipitation deficit was defined as the sum of SPI values over consecutive months with SPI values lower than -0.84.

In addition, the spatial extent of drought was defined to represent the total area impacted by drought. Given the uneven distribution of meteorological stations, a Thiessen polygon method was applied to approximate the representative area of each station. This method gives weights to individual stations according to the area represented by each (Jones and Hulme, 1996). The total surface area impacted by drought was calculated for Western Europe as a whole and for regions, including; central, south and north West Europe (Supplementary Figure 1). The total area impacted by drought was calculated for three different drought categories: mild drought: SPI = -0.84: return period of one in five years; moderate drought: SPI = -1.28: return period of one in 10 years; and severe drought: SPI = -1.65: return period of one in twenty years).

Trends in the SPI series, drought duration, magnitude and total surface area were assessed using least squares regression. For the SPI and drought area series, trends were

calculated using SPI-3 at 3-month intervals in February, May, August and November, which represent SPI-3 drought conditions during winter, spring, summer and autumn, respectively. SPI-12 in December was used to characterize drought at the annual scale. Trend significance was assessed using a modified version of the nonparametric Mann–Kendall statistic which limits the possible impact of serial autocorrelation on trend significance (Hamed and Ramachandra Rao, 1998). Significance was assessed at the 95% level ($p<0.05$).

Principal Component Analysis (PCA) was used to determine homogeneous regions in terms of drought variability. We applied an S-mode PCA using the SPI-12 series for each of the 199 stations. In the S-mode, stations are the variables and the time observations refer to the cases (Serrano *et al.*, 1999). As PCA is sensitive to missing values, we restricted our analysis to 1871-2018 when all 199 stations have complete records. The areas represented by each mode were identified by mapping the factorial loadings (i.e. the highest correlation found between each original variable and the extracted principal components). The loadings were interpolated by means of a method of splines with tension (Mitášová and Mitáš, 1993). The number of components was selected according to the criterion of eigenvalue > 1, before applying the Varimax rotation method to the original data. (White *et al.*, 1991). Once the components were rotated we retained those that grouped more than 75% of the total variance.

To extend the temporal analysis in each region, we identified the most representative station of each component (based on factorial loadings). The aim was to analyse the interannual variability of drought characteristics corresponding to each retained component from 1851 or 1861 onwards, according to data availability. Heat maps were plotted for each representative series based on the magnitude of change in drought series, based on linear regression. Trends were computed for running periods with a minimum of 30 and a maximum of 168 years, using annual (12-month) and seasonal (3-month) SPI values, as well as drought duration and magnitude series. Trend magnitude and significance in the heat maps correspond to the beginning of the period of analysis.

4. Results

4.1. Trend detection

Figure 3 illustrates the magnitude of change in long-term SPI series calculated at the annual scale (December SPI-12) and the corresponding statistical significance for our

three time periods. Statistically significant positive trends (wetter conditions) are evident over the British and Irish Isles and central Europe from 1851. On the contrary, albeit with fewer stations, negative trends (drier conditions) predominate over Italy and the Balkans. The negative trends in the Balkans are more pronounced from 1871 onwards, while the positive trends recorded from 1851 in northwest Europe are less consistent. In other regions like the Iberian Peninsula and southern France, no consistent patterns of change are evident, although negative trends prevail in western and southern Iberia since 1871 (Figure 3), albeit mostly non-significant at the 95% level ($p<0.05$). The percentage of stations with positive trends exceeds those with negative trends, irrespective of the season or the study period (Table 1).

Trends show important seasonal differences, analysed using SPI-3 (Supplementary Figures 2 to 5). Specifically, trends are mostly positive in winter, with largest change in central areas of west Europe. Exceptionally few stations exhibit statistically significant negative trends for winter. In spring, the spatial distribution of trends is more heterogeneous, with positive trends dominating in the British and Irish Isles, northern France and Germany and negative trends in the southwest of the Iberian Peninsula, Italy and the Balkans. However, in most cases (76.9% for the period 1871-2018), these trends were statistically non-significant at the 95% level ($p<0.05$).

Summer shows the largest percentage of negative trends, though statistically non-significant at the majority of stations. Significant negative trends are found mainly over the British and Irish Isles, particularly Ireland for the period 1871-2018. Trends are generally non-significant in autumn, however, we note a consistent positive trend in Ireland, and conversely a negative trend over northern parts of the Balkans.

Similar to SPI values, changes in drought duration and magnitude do not show consistent long-term trends across Western Europe (Figures 4 to 7 and Table 2). In a few instances, statistically significant positive or negative trends are observed at the seasonal scale (i.e. SPI-3, Figures 4 and 6). In contrast, no significant changes are noted for long-term droughts (i.e. SPI-12, Figures 5 and 7). For SPI-3, no coherent spatial patterns of drought trends are observed, with no clear differences even between northern and southern regions. As an indication of this high spatial variability in drought trends, using SPI-3 a significant positive trend in the duration and magnitude of droughts (i.e. a tendency towards longer/greater drought duration/magnitude) is observed for some stations in the Iberian Peninsula, the Balkans, Italy and the south of the British and Irish Isles. Conversely, a negative trend (i.e. less severe droughts) is noted in southern

Germany, Switzerland, eastern France, northern Ireland, Scotland and the Netherlands. Similarly, SPI-12 trends exhibit high spatial variability, even for neighbouring stations. Notably, few stations exhibit statistically significant trends (Figures 5 and 7).

The surface area impacted by drought does not show significant changes, at 3 and 12 month time scales (Figure 8). Changes are statistically significant only in winter, with a reduction of almost 3.6% in the area impacted by severe drought (SPI-3 < -1.28) between 1871 and 2018 (Table 3). The temporal evolution of the area impacted by drought reveals that the most extensive drought events were recorded in the 1870s, 1920s, 1940s, 1950s, 1970s and 2010s. This also suggests that interannual temporal variability clearly dominates over long-term trends. Focusing on northern and south west Europe, results indicate no clear significant trends (Supplementary Figures 6 and 7). In south west Europe, the most extensive droughts were recorded in the 1940s and 1950s, with severe droughts (SPI <-1.28) prevailing over more than 50% of the study domain. Severe drought was also extensive during the 1870s, 1890s, 2000s and 2010s, but with less of a spatial fingerprint by comparison with the 1940s and 1950s.

4.2. Spatial and temporal components of droughts

Given the spatial diversity of long-term SPI at the seasonal and annual time scale, we applied a PCA in an S-mode to delineate the main patterns of SPI-12 values from 1871-2018. Results suggest coherent spatial patterns, with clear linkages to the diversity of climate conditions across Western Europe (Figure 9). We retained 23 components, which together contribute more than 75.2% of the total variance. To illustrate the temporal variability corresponding to each component we selected the series with the highest correlation with each component as representative. The temporal evolution of SPI-12 for each representative series was explored for the period 1871-2018, and for the period 1851-2018 or 1861-2018 based on data availability.

Component 1 is representative of drought variability over Ireland (Figure 10), showing no clear long-term trend, with the exception of the summer SPI. While drought events are common over the whole series, the most severe droughts were observed during the 1850s, 1920s, 1930s, 1950s and 1970s. As illustrated in Figure 10, statistically significant trends are mainly placed close to the diagonal of the heat maps, which represent the results of the analysis over short periods of 30 years in duration. This suggests that only few significant trends are observed for long periods, and accordingly that short-term variability dominates over long-term trends. The only exception

corresponds to SPI-3 in summer, with a significant negative trend (the area in the plot framed by the dotted lines) noted for the periods of different duration (but in ~~allcases~~all cases for record lengths greater than 100 years) that start between 1880 and 1990 (in the X-axis) and finish between 2000 and 2018 (the Y-axis). This is depicted by the representative time series for this component (Cappoquinn station in Ireland).

Component 2 reveals the temporal variability of droughts in southern Germany, eastern France and most of Switzerland (Figure 11). This component is well-represented by the station of Karlsruhe in Germany, with the most severe droughts recorded in the 1850s, 1860s, 1900s, 1960s and 1970s. Significant trends are only found for winter from 1851 to 2018. Annual SPI exhibits a significant positive trend from 1860 to 2000. The duration and magnitude of droughts based on SPI-3 show a significant reduction from 1851 to 2018. This seems to be due to drought behaviour at the beginning of the series. These patterns are not defined using SPI-12, for which no significant trends are identified.

The third component is mostly representative of the temporal evolution of drought in southern England, best represented by the Althorp Park series. Major drought episodes are recorded in the 1850s, 1900s, 1920s, 1970s, 1990s and 2010s (Figure 12). Similar to the first and second components, no significant long-term trend is observed in this region. Significant trends are only found for short periods close to the diagonal of the heat maps for all the SPI, duration and magnitude series.

Component 4 captures the temporal variability of drought in northern Germany and the Netherlands (Figure 13), with the temporal evolution of drought illustrated using the series at Göttingen in Germany for the period 1861-2018. The most severe drought events are evident during the 1910s and 1930s. Again, this region does not show long-term trends in the various drought metrics examined. Significant trends are only found for short time spans (e.g. a negative trend from 1950 to 2000 during summer), but in spring it seems that there is a longer positive trend starting almost in 1900.

Component 5 represents drought variability over eastern Europe, including Hungary, eastern Austria, Slovakia and eastern Croatia. This is the only region which exhibits long-term changes in drought with two contrasting periods: a humid period from 1890 to 1930 and a persistent drought period from the 1960s onwards (Figure 14). Correspondingly, negative trends in the annual, winter and spring SPI, as well as in the drought duration and magnitude series, are evident from the beginning of the 20th century to present.

Component 6 summarizes drought variability in the majority of Italy and the western Balkans. This region experienced its main drought episodes during the 1920s and 1940s (Figure 15). In contrast, humid conditions dominate from the 1960s, especially in the past decade. Other drought metrics do not exhibit a significant long-term trend over this region. A similar temporal pattern is also noted for component 7 (Figure 16). In Iberia, the dominant role of natural variability is also noted, with drought conditions prevailing during the 1870s, 1880s, 1950s, 1990s and 2000s. Significant trends are restricted to summer SPI from the 1950s. However, the decrease in SPI values has no influence on the trends in drought duration and magnitude. In the northwestern UK, no long-term trends in the SPI series are observed. As illustrated in Figure 17, drought conditions predominated for the periods 1850-1900 and 1930-1980. On the other hand, humid conditions were more pronounced between 1900 and 1930 and from 1990 to 2018. Significant trends are recorded for different periods of 50-60 years, suggesting the influence of important long-term climate cycles.

Running trends in the SPI and drought indices for the components 9 to 23 are shown in Supplementary Figures 8 to 22. A quick inspection of these figures demonstrates that there are no clear long-term trends. This finding is evident for all components, including those corresponding to the Mediterranean region (e.g. Component 9 in Italy, Component 13 in northeastern Spain and southwestern France). In Barcelona, which is a representative of Component 13, dry conditions dominate from 2008, with no precedents since 1910. Nevertheless, more severe drought events were recorded between 1870 and 1905. In northern Spain (Component 14), no dominant long-term trends are observed, albeit with severe drought events between 1890 and 1920 and between 1980 and 2005. Exceptionally, a long term drying trend is recorded in southeastern Spain (Component 12). This trend is mostly impacted by the dominant humid conditions between 1880 and 1900. Thus, the recent dry periods recorded in the 1990s and 2010s can be seen as comparable to those recorded between 1910 and 1945 (Supplementary Figure 11). In other Mediterranean regions (e.g. Component 18, southern France), the last decades are mainly characterized by humid conditions. Conversely, the most severe droughts were recorded between 1915 and 1955 (Supplementary Figure 17). In Slovenia (Component 17), dominant dry conditions were mainly recorded in the past four decades, and earlier in the series between 1850 and 1940 (Supplementary Figure 16).

5. Discussion

This study presents the first comprehensive assessment of long-term variability and trends in drought over Western Europe, providing new perspectives on the severity of drought episodes over the instrumental period. Specifically, our assessment covers almost the whole of Western Europe and uses data from a relatively dense network of precipitation stations, which extend back to the mid 19th century. Previous studies have assessed long-term drought trends for specific regions in Europe (e.g. Noone *et al.*, 2017; Paulo *et al.*, 2016; Spraggs *et al.*, 2015; Todd *et al.*, 2013), or employed reconstruction approaches (e.g. Hanel *et al.*, 2018; Marvel *et al.*, 2019).

Our study stresses that from the long-term (1851-2018) perspective there are no generally consistent trends in droughts across Western Europe. This finding concurs with Lloyd-Hughes and Saunders (2002) and van der Schrier *et al.* (2006) who analyzed drought and moisture variability over Europe during the 20th century using gridded datasets. Exceptionally, long-term trends were detected in a few regions, mainly in eastern Europe and in Ireland during summer. In the remaining regions, the identified trends were only observed for short periods, suggesting high interdecadal variability of drought. This also indicates that anomalous drought episodes observed in Western Europe in the past two or three decades have several precedents, at least since 1850. This finding holds despite different climatic conditions prevailing in the region. For example, the increase of SPI values was generally the dominant pattern in some regions of northern Europe, with less frequent and severe drought events. In southern Europe, although the tendency towards more humid conditions was less evident, the long-term trend analysis did not suggest any tendency towards more severe droughts.

This finding seems to contradict previous studies that suggest an increase in drought severity over southern Europe in recent decades (e.g. Gudmundsson and Seneviratne, 2016; Hoerling *et al.*, 2012; Stagge *et al.*, 2017; Vicente-Serrano *et al.*, 2014c). These differences might be simply explained by differences in study period. This issue is of particular importance in trend detection, given that the magnitude and significance of the observed trends can vary considerably, as a function of the length of the series and the selected study period (Hannaford *et al.*, 2013; Murphy *et al.*, 2013). The possible effect of the selection of the study period is particularly evident for Component 13, represented by the observatory of Barcelona, where no significant climate signal was observed due to the presence of longer and more severe droughts in the earlier decades

of the series. This highlights the importance of conducting trend assessments using long-term data and the importance of ongoing national and international data rescue initiatives (Brunet and Jones, 2011; Ryan *et al.*, 2018).

We emphasise that our findings should be seen in the context of the drought metric applied. Our assessment of drought characteristics is based on SPI, which is a precipitation-based metric. For a long-term assessment of drought in the region, it is not possible to use metrics that employ other important variables (e.g. streamflow, soil moisture or AED). This is simply due to data scarcity of these variables. For example, streamflow data are available, with adequate density, only for the last few decades (Blöschl *et al.*, 2019; Vicente-Serrano *et al.*, 2019). This is also the case for the large number of meteorological variables necessary to quantify AED (e.g. wind speed, relative humidity and solar radiation). Studies that have analyzed long-term drought trends using hydrological metrics, are based on reconstructions and model simulations (Hanel *et al.*, 2018), which have large uncertainty (Cheng *et al.*, 2017; Stegehuis *et al.*, 2013). Thus, the lack of trends presented in our study, should be seen within the context of our study design.

It is necessary to stress that this study may be affected by some limitations. For example, Murphy *et al.*, (2019, 2020) have shown that pre 1870 winter precipitation in north West Europe is likely too low due to undercatch of snow. Such changes that affect multiple stations simultaneously may not be detected using relative homogenisation methods and they could affect winter and annual SPI trends for stations in the British and Irish Isles. Moreover, the unequal distribution of gauges could affect the obtained drought patterns, mostly for southern Europe in which spatial differences in the drought evolution are stronger. In any case, the unequal station coverage would not affect the intended application of the PCA in this study, which was not intended to represent the main patterns of drought variability but to identify regions with homogeneous behavior allowing for a more straightforward analysis of the long-term variability and trends.

Our findings do not necessarily contradict several recent works that have indicated an increase in the frequency, severity and duration of droughts in Western Europe in recent decades. For example, according to Robinson *et al.* (2017), AED has significantly increased in northern West Europe over the last decades. A similar finding has also been confirmed by Vicente-Serrano *et al.* (2014a) for southern Europe, being mostly associated with an increase in air temperature and decline in relative humidity. Some studies indicate that streamflow variability has been generally less impacted by the

increase in AED (Vicente-Serrano *et al*., 2019), mainly due to the stronger response of streamflow to precipitation than to AED (Yang *et al.*, 2018). Nonetheless, changes in AED could have more influence on drought in regions impacted by strong land cover changes (e.g. southern Europe). In such environments, natural revegetation in humid headwaters and the generation of new irrigated lands (García-Ruiz *et al.*, 2011) could favour higher evapotranspiration under enhanced AED and accordingly increase hydrological drought conditions downstream (Vicente-Serrano *et al.*, 2017). In addition, increased AED would enhance the severity of droughts associated with precipitation deficit. Recently, this dependency has been confirmed by García-Herrera *et al.* (2019) for the 2016/2017 drought event in Europe. Several ecological studies have reported an enhancement of drought impacts during recent decades in some European regions, albeit with no significant precipitation changes (e.g. Carnicer *et al.*, 2011; Peñuelas *et al.*, 2018; Vicente-Serrano *et al.*, 2012). Enhanced AED serves to increase vegetation stress during periods of negative soil moisture anomalies, irrespective of the vapor pressure deficit control on stomatal conductance (Zhang *et al.*, 2019). This situation would reduce biomass production and increase the risk of forest mortality (Allen *et al.*, 2015; Vicente-Serrano *et al.*, 2019a and c). In this context, the findings of this study stress that although the increase of drought severity and its environmental and/or hydrological impacts cannot be supported by the decrease in precipitation; it is likely they are more linked to human transformations (e.g. irrigation, land cover changes, etc.) or to observed increases in AED under global warming (Vicente-Serrano *et al.*, 2020a). The thermodynamic processes associated with an AED enhancement in recent decades are intense in the region (Hirschi *et al.*, 2011; Seneviratne *et al.*, 2010; Teuling *et al.*, 2013). Herein, what are termed "global-change-type-droughts" by Breshears *et al.* (2005) to refer to drought episodes under global warming, seems to be representative of possible drought intensification in Western Europe in recent decades, associated with warming conditions and related thermodynamic processes and feedbacks. Thus, it can be concluded that drought intensification in Western Europe cannot be attributed to precipitation deficit, at least in the last 170 years.

With respect to those studies that usually classify Europe into large domains (e.g. northern vs. southern Europe) in order to characterize drought variability and trends, our study indicates that this approach has a degree of uncertainty, recalling the strong spatial variability of drought. The principal component analysis showed consistent spatial patterns of drought, whose temporal variability was homogenous. However, the

temporal variability of drought showed considerable differences amongst neighbouring regions. This strong spatial and temporal variability was identified at the regional scale in Europe, including Spain (e.g. Vicente-Serrano, 2006b; Vicente-Serrano *et al.*, 2004), Portugal (e.g. Santos *et al.*, 2010), Italy (e.g. Bonaccorso *et al.*, 2003) and Serbia (e.g. Gocic and Trajkovic, 2014), amongst others. This strong variability is mainly attributed to the complex atmospheric configurations that control climate in the region. In this context, although the North Atlantic Oscillation (NAO) is the dominant circulation pattern controlling drought variability in Europe (López-Moreno *et al.*, 2008), other large-scale circulation patterns also contribute to climate variability in specific European regions (Kingston *et al.*, 2015; Manzano *et al.*, 2019; Trigo *et al.*, 2009; Vicente-Serrano *et al.*, 2016). This is more pronounced in the Mediterranean, where the influence of local/regional circulation variability induces more heterogeneous drought patterns, even for small areas (Vicente-Serrano and López-Moreno, 2006).

6. Conclusions

This study stresses the following findings:

- Spatial differences were observed in the SPI12 magnitude trend, where a positive trend was found in the British and Irish Isles, northern France and Germany, and a negative trend in the southeast of the Iberian Peninsula, Italy and Balkans. In addition, this great spatial variability is reflected in the 23 components of the PCA to obtain 75.2% of the variance explained.
- Seasonal differences were found in the SPI3 magnitude trend, where a negative trend in summer was detected, especially in the British and Irish Isles. In addition, a reduction in the area affected by severe drought was detected, especially in winter.
- With few exceptions, trends in droughts over Western Europe are statistically non-significant from a long-term perspective.
- Changes in droughts are spatially variable, especially on a seasonal basis. Therefore detailed local and regional assessment of drought variability should be of high priority in Western Europe. Such assessments would provide local policy and decision-makers with the most appropriate and reliable information for understanding drought change and management.

Acknowledgements

This work was supported by the research projects PCIN-2015-220 and CGL2017-82216-R financed by the Spanish Commission of Science and Technology and FEDER, IMDROFLOOD financed by the WaterWorks 2014 co-funded call of the European Commission, CROSSDRO financed by the AXIS (Assessment of Cross(X) - sectorial climate Impacts and pathways for Sustainable transformation) JPI-Climate co-funded call of the European Commission, INDECIS, which is part of ERA4CS, an ERA-NET initiated by JPI Climate, and funded by FORMAS (SE), DLR (DE), BMWFW (AT), IFD (DK), MINECO (ES), ANR (FR), FCT (PT) with co-funding by the European Union (Grant 690462), Irish Research Council COALESCE grant (COALESCE/2019/43). Dhais Peña-Angulo received a "Juan de la Cierva" postdoctoral contract (FJCI-2017-33652 Spanish Ministry of Economy and Competitiveness, MEC), Marco Turco has received funding from the Spanish Ministry of Science, Innovation and Universities through the project PREDFIRE (RTI2018-099711-J-I00). Our grateful thanks extend to Instituto Português do Mar e da Atmosfera-(IPMA), Portugal, Agencia Estatal de Meteorología (AEMET), Spain, Deutscher Wetterdienst (Germany), Meteofrance (France), Met Office (UK), Koninklijk Nederlands Meteorologisch Instituut (KNMI), Netherlands, the Global Historical Climatology Network (GHCN), and the European Climate Assessment & Dataset (ECAD) for providing precipitation data used in this study.

References

Allen CD, Breshears DD, McDowell NG. 2015. On underestimation of global vulnerability to tree mortality and forest die-off from hotter drought in the Anthropocene. *Ecosphere* **6**(8). DOI: 10.1890/ES15-00203.1.

Beguería S, Vicente-Serrano SM, Reig F, Latorre B. 2014. Standardized precipitation evapotranspiration index (SPEI) revisited: Parameter fitting, evapotranspiration models, tools, datasets and drought monitoring. *International Journal of Climatology* **34**(10). DOI: 10.1002/joc.3887.

Beniston M, Stephenson DB, Christensen OB, Ferro CAT, Frei C, Goyette S, Halsnaes K, Holt T, Jylhä K, Koffi B, Palutikof J, Schöll R, Semmler T, Woth K. 2007. Future extreme events in European climate: An exploration of regional climate model

projections. *Climatic Change* **81**(SUPPL. 1): 71–95. DOI: 10.1007/s10584-006-9226-z.
Blöschl G, Hall J, Viglione A, Perdigão RAP, Parajka J, Merz B, Lun D, Arheimer B, Aronica GT, Bilibashi A, Boháč M, Bonacci O, Borga M, Čanjevac I, Castellarin A, Chirico GB, Claps P, Frolova N, Ganora D, Gorbachova L, Gül A, Hannaford J, Harrigan S, Kireeva M, Kiss A, Kjeldsen TR, Kohnová S, Koskela JJ, Ledvinka O, Macdonald N, Mavrova-Guirguinova M, Mediero L, Merz R, Molnar P, Montanari A, Murphy C, Osuch M, Ovcharuk V, Radevski I, Salinas JL, Sauquet E, Šraj M, Szolgay J, Volpi E, Wilson D, Zaimi K, Živković N. 2019. Changing climate both increases and decreases European river floods. *Nature* **573**(7772): 108–111. DOI: 10.1038/s41586-019-1495-6.
Bonaccorso B, Bordi I, Cancelliere A, Rossi G, Sutera A. 2003. Spatial variability of drought: An analysis of the SPI in Sicily. *Water Resources Management*, 273–296.
Bordi I, Fraedrich K, Sutera A. 2009. Observed drought and wetness trends in Europe: An update. *Hydrology and Earth System Sciences*, 1519–1530.
Brázdil R, Trnka M, Mikšovský J, Řezníčková L, Dobrovolný P. 2015. Spring-summer droughts in the Czech Land in 1805-2012 and their forcings. *International Journal of Climatology*, 1405–1421.
Breshears DD, Cobb NS, Rich PM, Price KP, Allen CD, Balice RG, Romme WH, Kastens JH, Floyd ML, Belnap J, Anderson JJ, Myers OB, Meyer CW. 2005. Regional vegetation die-off in response to global-change-type drought. *Proceedings of the National Academy of Sciences of the United States of America* **102**(42): 15144–15148. DOI: 10.1073/pnas.0505734102.
Briffa KR, van der Schrier G, Jones PD. 2009. Wet and dry summers in europe since 1750: Evidence of increasing drought. *International Journal of Climatology*, 1894–1905.
Brunet M, Jones P. 2011. Data rescue initiatives: Bringing historical climate data into the 21st century. *Climate Research* **47**: 29–40. DOI: 10.3354/cr00960.
Carnicer J, Coll M, Ninyerola M, Pons X, Sánchez G, Peñuelas J. 2011. Widespread crown condition decline, food web disruption, and amplified tree mortality with increased climate change-type drought. *Proceedings of the National Academy of Sciences of the United States of America* **108**(4): 1474–1478. DOI: 10.1073/pnas.1010070108.
Cheng S, Huang J, Ji F, Lin L. 2017. Uncertainties of soil moisture in historical simulations and future projections. *Journal of Geophysical Research: Atmospheres*.

John Wiley & Sons, Ltd **122**(4): 2239–2253. DOI: 10.1002/2016JD025871.

Cindrić K, Telišman Prtenjak M, Herceg-Bulić I, Mihajlović D, Pasarić Z. 2016. Analysis of the extraordinary 2011/2012 drought in Croatia. *Theoretical and Applied Climatology*, 503–522.

Di Lena B, Vergni L, Antenucci F, Todisco F, Mannocchi F. 2014. Analysis of drought in the region of Abruzzo (Central Italy) by the Standardized Precipitation Index. *Theoretical and Applied Climatology*, 41–52.

Domínguez-Castro F, Vicente-Serrano SM, Tomás-Burguera M, Peña-Gallardo M, Beguería S, El Kenawy A, Luna Y, Morata A. 2019. High spatial resolution climatology of drought events for Spain: 1961–2014. *International Journal of Climatology* **0**(0). DOI: 10.1002/joc.6126.

Forzieri G, Feyen L, Rojas R, Flörke M, Wimmer F, Bianchi A. 2014. Ensemble projections of future streamflow droughts in Europe. *Hydrology and Earth System Sciences* **18**(1): 85–108. DOI: 10.5194/hess-18-85-2014.

García-Herrera R, Garrido-Pérez, J.M. Barriopedro D, Ordóñez C, Vicente-Serrano, S.M. Nieto R, Gimeno L, Sorí R, Yiou P. 2019. The European 2016/2017 drought. *Journal of Climate* **32**: 3169–3187.

García-Herrera R, Paredes D, Trigo RM, Trigo IF, Hernández E, Barriopedro D, Mendes MA. 2007. The outstanding 2004/05 drought in the Iberian Peninsula: Associated atmospheric circulation. *Journal of Hydrometeorology*, 483–498.

García-Ruiz JM, López-Moreno JI, Vicente-Serrano SM, Lasanta-Martínez T, Beguería S. 2011. Mediterranean water resources in a global change scenario. *Earth-Science Reviews* **105**(3–4). DOI: 10.1016/j.earscirev.2011.01.006.

Gocic M, Trajkovic S. 2014. Spatiotemporal characteristics of drought in Serbia. *Journal of Hydrology*, 110–123.

Gudmundsson L, Seneviratne SI. 2016. Anthropogenic climate change affects meteorological drought risk in Europe. *Environmental Research Letters* **11**(4). DOI: 10.1088/1748-9326/11/4/044005.

Gudmundsson L, Seneviratne SI, Zhang X. 2017. Anthropogenic climate change detected in European renewable freshwater resources. *Nature Climate Change* **7**(11): 813–816. DOI: 10.1038/nclimate3416.

Hamed KH, Ramachandra Rao A. 1998. A modified Mann-Kendall trend test for autocorrelated data. *Journal of Hydrology* **204**(1–4): 182–196. DOI: 10.1016/S0022-1694(97)00125-X.

Hanel M, Rakovec O, Markonis Y, Máca P, Samaniego L, Kyselý J, Kumar R. 2018. Revisiting the recent European droughts from a long-term perspective. *Scientific Reports* **8**(1). DOI: 10.1038/s41598-018-27464-4.

Hannaford J, Buys G, Stahl K, Tallaksen LM. 2013. The influence of decadal-scale variability on trends in long European streamflow records. *Hydrology and Earth System Sciences* **17**(7): 2717–2733. DOI: 10.5194/hess-17-2717-2013.

Hayes M, Svoboda M, Wall N, Widhalm M. 2011. The lincoln declaration on drought indices: Universal meteorological drought index recommended. *Bulletin of the American Meteorological Society* **92**(4): 485–488. DOI: 10.1175/2010BAMS3103.1.

Hirschi M, Seneviratne SI, Alexandrov V, Boberg F, Boroneant C, Christensen OB, Formayer H, Orlowsky B, Stepanek P. 2011. Observational evidence for soil-moisture impact on hot extremes in southeastern Europe. *Nature Geoscience* **4**(1): 17–21. DOI: 10.1038/ngeo1032.

Hisdal H, Stahl K, Tallaksen LM, Demuth S. 2001. Have streamflow droughts in Europe become more severe or frequent? *International Journal of Climatology* **21**(3): 317–333. DOI: 10.1002/joc.619.

Hoerling M, Eischeid J, Perlwitz J, Quan X, Zhang T, Pegion P, Hoerling M, Eischeid J, Perlwitz J, Quan X, Zhang T, Pegion P. 2012. On the Increased Frequency of Mediterranean Drought. *Journal of Climate* **25**(6): 2146–2161. DOI: 10.1175/JCLI-D-11-00296.1.

Hoy A, Hänsel S, Skalak P, Ustrnul Z, Bochníček O. 2017. The extreme European summer of 2015 in a long-term perspective. *International Journal of Climatology*, 943–962.

Ionita M, Tallaksen LM, Kingston DG, Stagge JH, Laaha G, Van Lanen HAJ, Scholz P, Chelcea SM, Haslinger K. 2017. The European 2015 drought from a climatological perspective. *Hydrology and Earth System Sciences*, 1397–1419.

Jones PD, Hulme M. 1996. Calculating regional climatic time series for temperature and precipitation: methods and illustrations. *International Journal of Climatology*. John Wiley & Sons, Ltd **16**(4): 361–377. DOI: 10.1002/(SICI)1097-0088(199604)16:4<361::AID-JOC53>3.0.CO;2-F.

Kingston DG, Stagge JH, Tallaksen LM, Hannah DM. 2015. European-scale drought: Understanding connections between atmospheric circulation and meteorological drought indices. *Journal of Climate* **28**(2): 505–516. DOI: 10.1175/JCLI-D-14-00001.1.

Laaha G, Gauster T, Tallaksen LM, Vidal J-P, Stahl K, Prudhomme C, Heudorfer B,

644 Vlnas R, Ionita M, Van Lanen HAJ, Adler M-J, Caillouet L, Delus C, Fendekova M,
645 Gailliez S, Hannaford J, Kingston D, Van Loon AF, Mediero L, Osuch M, Romanowicz
646 R, Sauquet E, Stagge JH, Wong WK. 2017. The European~2015 drought from a
647 hydrological perspective. *Hydrology and Earth System Sciences* **21**(6): 3001–3024.
648 DOI: 10.5194/hess-21-3001-2017.
649 Lloyd-Hughes B. 2014. The impracticality of a universal drought definition. *Theoretical*
650 *and Applied Climatology* **117**(3–4): 607–611. DOI: 10.1007/s00704-013-1025-7.
651 Lloyd-Hughes B, Saunders MA. 2002. A drought climatology for Europe. *International*
652 *Journal of Climatology*. John Wiley & Sons, Ltd. **22**(13): 1571–1592. DOI:
653 10.1002/joc.846.
654 López-Moreno JI, Vicente-Serrano SM, López-Moreno JI, Vicente-Serrano SM. 2008.
655 Positive and Negative Phases of the Wintertime North Atlantic Oscillation and Drought
656 Occurrence over Europe: A Multitemporal-Scale Approach. *Journal of Climate* **21**(6):
657 1220–1243. DOI: 10.1175/2007JCLI1739.1.
658 Lorenzo-Lacruz J, Garcia C, Morán-Tejeda E. 2017. Groundwater level responses to
659 precipitation variability in Mediterranean insular aquifers. *Journal of Hydrology*.
660 Elsevier **552**: 516–531. DOI: 10.1016/J.JHYDROL.2017.07.011.
661 Lorenzo-Lacruz J, Morán-Tejeda E, Vicente-Serrano SM, López-Moreno JI. 2013.
662 Streamflow droughts in the Iberian Peninsula between 1945 and 2005: spatial and
663 temporal patterns. *Hydrology and Earth System Sciences* **17**(1): 119–134. DOI:
664 10.5194/hess-17-119-2013.
665 Manzano A, Clemente MA, Morata A, Luna MY, Beguería S, Vicente-Serrano SM,
666 Martín ML. 2019. Analysis of the atmospheric circulation pattern effects over SPEI
667 drought index in Spain. *Atmospheric Research* **230**: 104630. DOI:
668 https://doi.org/10.1016/j.atmosres.2019.104630.
669 Marchant BP, Bloomfield JP. 2018. Spatio-temporal modelling of the status of
670 groundwater droughts. *Journal of Hydrology* **564**: 397–413. DOI:
671 10.1016/j.jhydrol.2018.07.009.
672 Martins DS, Raziei T, Paulo AA, Pereira LS. 2012. Spatial and temporal variability of
673 precipitation and drought in Portugal. *Natural Hazards and Earth System Science*,
674 1493–1501.
675 Marvel K, Cook BI, Bonfils CJW, Durack PJ, Smerdon JE, Williams AP. 2019.
676 Twentieth-century hydroclimate changes consistent with human influence. *Nature*, 59–
677 65.

Mckee TB, Doesken NJ, Kleist J. 1993. The relationshio of drought frequency and duration to time scales. *Eighth Conference on Applied Climatology* 17–22.

Merino A, López L, Hermida L, Sánchez JL, García-Ortega E, Gascón E, Fernández-González S. 2015. Identification of drought phases in a 110-year record from Western Mediterranean basin: Trends, anomalies and periodicity analysis for Iberian Peninsula. *Global and Planetary Change*, 96–108.

Mestre O, Domonkos P, Picard F, Auer I, Robin S, Lebarbier E, Boehm R, Aguilar E, Guijarro J, Vertachnik G, Klančar M, Dubuisson B, Stepanek P. 2013. HOMER: A homogenization software - methods and applications. *Idojaras* **117**.

Mihajlović D. 2006. Monitoring the 2003-2004 meteorological drought over Pannonian part of Croatia. *International Journal of Climatology*, 2213–2225.

Mitášová H, Mitáš L. 1993. Interpolation by regularized spline with tension: I. Theory and implementation. *Mathematical Geology* **25**(6): 641–655. DOI: 10.1007/BF00893171.

Moravec V, Markonis Y, Rakovec O, Kumar R, Hanel M. 2019. A 250-Year European Drought Inventory Derived From Ensemble Hydrologic Modeling. *Geophysical Research Letters*, 5909–5917.

Murphy C, Harrigan S, Hall J, Wilby RL. 2013. Climate-driven trends in mean and high flows from a network of reference stations in Ireland | Tendances induites par le climat dans les séries de débits moyens et élevés à partir d'un réseau de stations de référence en Irlande. *Hydrological Sciences Journal* **58**(4): 755–772. DOI: 10.1080/02626667.2013.782407.

Murphy C, Wilby RL, Matthews T, Horvath C, Crampsie A, Ludlow F, Noone S, Brannigan J, Hannaford J, McLeman R, Jobbova E. 2020. The forgotten drought of 1765–1768: Reconstructing and re-evaluating historical droughts in the British and Irish Isles. *International Journal of Climatology*. John Wiley & Sons, Ltd **n/a**(n/a). DOI: 10.1002/joc.6521.

Murphy C, Wilby RL, Matthews TKR, Thorne P, Broderick C, Fealy R, Hall J, Harrigan S, Jones P, McCarthy G, MacDonald N, Noone S, Ryan C. 2019. Multi-century trends to wetter winters and drier summers in the England and Wales precipitation series explained by observational and sampling bias in early records. *International Journal of Climatology*. DOI: 10.1002/joc.6208.

Nicault A, Alleaume S, Brewer S, Carrer M, Nola P, Guiot J. 2008. Mediterranean drought fluctuation during the last 500 years based on tree-ring data. *Climate Dynamics*

712 **31**(2–3): 227–245. DOI: 10.1007/s00382-007-0349-3.
713 Noone S, Broderick C, Duffy C, Matthews T, Wilby RL, Murphy C. 2017. A 250-year
714 drought catalogue for the island of Ireland (1765–2015). *International Journal of*
715 *Climatology* **37**: 239–254. DOI: 10.1002/joc.4999.
716 Noone S, Murphy C, Coll J, Matthews T, Mullan D, Wilby RL, Walsh S. 2016.
717 Homogenization and analysis of an expanded long-term monthly rainfall network for
718 the Island of Ireland (1850–2010). *International Journal of Climatology* **36**(8): 2837–
719 2853. DOI: 10.1002/joc.4522.
720 Parry S, Hannaford J, Lloyd-Hughes B, Prudhomme C. 2012. Multi-year droughts in
721 Europe: Analysis of development and causes. *Hydrology Research* **43**(5): 689–706.
722 DOI: 10.2166/nh.2012.024.
723 Paulo A, Martins D, Pereira LS. 2016. Influence of Precipitation Changes on the SPI
724 and Related Drought Severity. An Analysis Using Long-Term Data Series. *Water*
725 *Resources Management*, 5737–5757.
726 Peñuelas J, Sardans J, Filella I, Estiarte M, Llusià J, Ogaya R, Carnicer J, Bartrons M,
727 Rivas-Ubach A, Grau O, Peguero G, Margalef O, Pla-Rabés S, Stefanescu C, Asensio
728 D, Preece C, Liu L, Verger A, Rico L, Barbeta A, Achotegui-Castells A, Gargallo-
729 Garriga A, Sperlich D, Farré-Armengol G, Fernández-Martínez M, Liu D, Zhang C,
730 Urbina I, Camino M, Vives M, Nadal-Sala D, Sabaté S, Gracia C, Terradas J. 2018.
731 Assessment of the impacts of climate change on Mediterranean terrestrial ecosystems
732 based on data from field experiments and long-term monitored field gradients in
733 Catalonia. *Environmental and Experimental Botany* **152**: 49–59. DOI:
734 10.1016/j.envexpbot.2017.05.012.
735 Potop V, Boroneanț C, Možný M, Štěpánek P, Skalák P. 2014. Observed spatiotemporal
736 characteristics of drought on various time scales over the Czech Republic. *Theoretical*
737 *and Applied Climatology*, 563–581.
738 Robinson EL, Blyth EM, Clark DB, Finch J, Rudd AC. 2017. Trends in atmospheric
739 evaporative demand in Great Britain using high-resolution meteorological data.
740 *Hydrology and Earth System Sciences* **21**(2): 1189–1224. DOI: 10.5194/hess-21-1189-
741 2017.
742 Ryan C, Duffy C, Broderick C, Thorne PW, Curley M, Walsh S, Daly C, Treanor M,
743 Murphy C. 2018. Integrating Data Rescue into the Classroom. *Bulletin of the American*
744 *Meteorological Society* **99**(9): 1757–1764. DOI: 10.1175/BAMS-D-17-0147.1.
745 Samaniego L, Thober S, Kumar R, Wanders N, Rakovec O, Pan M, Zink M, Sheffield J,

Wood EF, Marx A. 2018. Anthropogenic warming exacerbates European soil moisture droughts. *Nature Climate Change* **8**(5): 421–426. DOI: 10.1038/s41558-018-0138-5.

Santos J, Corte-Real J, Leite S. 2007. Atmospheric large-scale dynamics during the 2004/2005 winter drought in Portugal. *International Journal of Climatology*, 571–586.

Santos JF, Pulido-Calvo I, Portela MM. 2010. Spatial and temporal variability of droughts in Portugal. *Water Resources Research*.

Seneviratne SI, Corti T, Davin EL, Hirschi M, Jaeger EB, Lehner I, Orlowsky B, Teuling AJ. 2010. Investigating soil moisture-climate interactions in a changing climate: A review. *Earth-Science Reviews* **99**(3–4): 125–161. DOI: 10.1016/j.earscirev.2010.02.004.

Serrano A, García J, Mateos VL, Cancillo ML, Garrido J. 1999. Monthly Modes of Variation of Precipitation over the Iberian Peninsula. *Journal of Climate* **12**(9): 2894–2919. DOI: 10.1175/1520-0442(1999)012<2894:MMOVOP>2.0.CO;2.

Sheffield J, Wood EF. 2008. Projected changes in drought occurrence under future global warming from multi-model, multi-scenario, IPCC AR4 simulations. *Climate Dynamics*, 79–105.

Sousa PM, Trigo RM, Aizpurua P, Nieto R, Gimeno L, Garcia-Herrera R. 2011. Trends and extremes of drought indices throughout the 20th century in the Mediterranean. *Natural Hazards and Earth System Science* **11**(1): 33–51. DOI: 10.5194/nhess-11-33-2011.

Spinoni J, Barbosa P, De Jager A, McCormick N, Naumann G, Vogt J V., Magni D, Masante D, Mazzeschi M. 2019. A new global database of meteorological drought events from 1951 to 2016. *Journal of Hydrology: Regional Studies*. Elsevier **22**: 100593. DOI: 10.1016/J.EJRH.2019.100593.

Spinoni J, Naumann G, Vogt J, Barbosa P. 2015. European drought climatologies and trends based on a multi-indicator approach. *Global and Planetary Change*, 50–57.

Spinoni J, Naumann G, Vogt JV. 2017. Pan-European seasonal trends and recent changes of drought frequency and severity. *Global and Planetary Change* **148**: 113–130. DOI: 10.1016/j.gloplacha.2016.11.013.

Spinoni J, Vogt J V, Naumann G, Barbosa P, Dosio A. 2018. Will drought events become more frequent and severe in Europe? *International Journal of Climatology* **38**(4): 1718–1736. DOI: 10.1002/joc.5291.

Spraggs G, Peaver L, Jones P, Ede P. 2015. Re-construction of historic drought in the Anglian Region (UK) over the period 1798-2010 and the implications for water

780 resources and drought management. *Journal of Hydrology*, 231–252.
781 Stagge JH, Kingston DG, Tallaksen LM, Hannah DM. 2017. Observed drought indices
782 show increasing divergence across Europe. *Scientific Reports* **7**(1). DOI:
783 10.1038/s41598-017-14283-2.
784 Stegehuis AI, Vautard R, Ciais P, Teuling AJ, Jung M, Yiou P. 2013. Summer
785 temperatures in Europe and land heat fluxes in observation-based data and regional
786 climate model simulations. *Climate Dynamics* **41**(2): 455–477. DOI: 10.1007/s00382-
787 012-1559-x.
788 Tallaksen LM, Hisdal H, Van Lanen H. 2009. Space-time modeling of catchment scale
789 drought characteristics. *Journal of Hydrology* **375**: 363–372. DOI:
790 10.1016/j.jhydrol.2009.06.032.
791 Tallaksen LM, Madsen H, Clausen B. 1997. On the definition and modelling of
792 streamflow drought duration and deficit volume. *Hydrological Sciences Journal*. Taylor
793 & Francis Group **42**(1): 15–33. DOI: 10.1080/02626669709492003.
794 Teuling AJ, Van Loon AF, Seneviratne SI, Lehner I, Aubinet M, Heinesch B, Bernhofer
795 C, Grünwald T, Prasse H, Spank U. 2013. Evapotranspiration amplifies European
796 summer drought. *Geophysical Research Letters* **40**(10): 2071–2075. DOI:
797 10.1002/grl.50495.
798 Todd B, Macdonald N, Chiverrell RC. 2015. Revision and extension of the composite
799 Carlisle rainfall record, northwest England: 1757-2012. *International Journal of*
800 *Climatology* **35**(12): 3593–3607. DOI: 10.1002/joc.4233.
801 Todd B, Macdonald N, Chiverrell RC, Caminade C, Hooke JM. 2013. Severity,
802 duration and frequency of drought in SE England from 1697 to 2011. *Climatic Change*,
803 673–687.
804 Trigo R, Valente M, Trigo I, Miranda P, Ramos A, Paredes D, García-Herrera R. 2009.
805 The Impact of North Atlantic Wind and Cyclone Trends on European Precipitation and
806 Significant Wave Height in the Atlantic. *Annals of the New York Academy of Sciences*
807 **1146**: 212–234. DOI: 10.1196/annals.1446.014.
808 Trigo RM, Añel JA, Barriopedro D, García-Herrera R, Gimeno L, Nieto R, Castillo R,
809 Allen MR, Massey N. 2013. The Record Winter Drought of 2011 – 12 in the Iberian
810 Peninsula. *American Meteorological Society* (September): 41–45.
811 van der Schrier G, Briffa KR, Jones PD, Osborn TJ. 2006. Summer moisture variability
812 across Europe. *Journal of Climate*, 2818–2834.
813 Venema VKC, Mestre O, Aguilar E, Auer I, Guijarro JA, Domonkos P, Vertacnik G,

Szentimrey T, Stepanek P, Zahradnicek P, Viarre J, Müller-Westermeier G, Lakatos M, Williams CN, Menne MJ, Lindau R, Rasol D, Rustemeier E, Kolokythas K, Marinova T, Andresen L, Acquaotta F, Fratianni S, Cheval S, Klancar M, Brunetti M, Gruber C, Prohom Duran M, Likso T, Esteban P, Brandsma T. 2012. Benchmarking homogenization algorithms for monthly data. *Climate of the Past* **8**(1): 89–115. DOI: 10.5194/cp-8-89-2012.

Vicente-Serrano SM. 2006a. Spatial and temporal analysis of droughts in the Iberian Peninsula (1910–2000). *Hydrological Sciences Journal*. Taylor & Francis Group **51**(1): 83–97. DOI: 10.1623/hysj.51.1.83.

Vicente-Serrano SM. 2006b. Differences in spatial patterns of drought on different time scales: An analysis of the Iberian Peninsula. *Water Resources Management* **20**(1). DOI: 10.1007/s11269-006-2974-8.

Vicente-Serrano SM. 2016. Foreword: Drought complexity and assessment under climate change conditions. *Cuadernos de Investigacion Geografica* **42**(1). DOI: 10.18172/cig.2961.

Vicente-Serrano SM, Azorin-Molina C, Sanchez-Lorenzo A, Revuelto J, López-Moreno JI, González-Hidalgo JC, Moran-Tejeda E, Espejo F. 2014a. Reference evapotranspiration variability and trends in Spain, 1961-2011. *Global and Planetary Change* **121**: 26–40. DOI: 10.1016/j.gloplacha.2014.06.005.

Vicente-Serrano SM, García-Herrera R, Barriopedro D, Azorin-Molina C, López-Moreno JI, Martín-Hernández N, Tomás-Burguera M, Gimeno L, Nieto R. 2016. The Westerly Index as complementary indicator of the North Atlantic oscillation in explaining drought variability across Europe. *Climate Dynamics* **47**(3–4). DOI: 10.1007/s00382-015-2875-8.

Vicente-Serrano SM, González-Hidalgo JC, de Luis M, Raventós J. 2004. Drought patterns in the Mediterranean area: The Valencia region (eastern Spain). *Climate Research* **26**(1). DOI: 10.3354/cr026005.

Vicente-Serrano SM, Lopez-Moreno J-I, Beguería S, Lorenzo-Lacruz J, Sanchez-Lorenzo A, García-Ruiz JM, Azorin-Molina C, Morán-Tejeda E, Revuelto J, Trigo R, Coelho F, Espejo F. 2014b. Evidence of increasing drought severity caused by temperature rise in southern Europe. *Environmental Research Letters* **9**(4): 044001. DOI: 10.1088/1748-9326/9/4/044001.

Vicente-Serrano SM, López-Moreno JI. 2006. The influence of atmospheric circulation at different spatial scales on winter drought variability through a semi-arid climatic

gradient in Northeast Spain. *International Journal of Climatology* **26**(11). DOI: 10.1002/joc.1387.

Vicente-Serrano SM, McVicar T, Miralles D, Yang Y, Tomas-Burguera M. 2020a. Unravelling the influence of atmospheric evaporative demand on drought under climate dynamics. *Wiley Interdisciplinary Reviews: Climate Change* **in press**.

Vicente-Serrano SM, Peña-Gallardo M, Hannaford J, Murphy C, Lorenzo-Lacruz J, Dominguez-Castro F, López-Moreno J, Beguería S, Noguera I, Harrigan S, Vidal J-P. 2019. Climate, irrigation, and land-cover change explain streamflow trends in countries bordering the Northeast Atlantic. *Geophysical Research Letters* **46**: 10821–10833.

Vicente-Serrano SM, Quiring S, Peña-Gallardo M, Domínguez-castro F, Yuan S. 2020b. A review of environmental droughts: Increased risk under global warming? *Earth Science Reviews*.

Vicente-Serrano SM, Zouber A, Lasanta T, Pueyo Y. 2012. Dryness is accelerating degradation of vulnerable shrublands in semiarid mediterranean environments. *Ecological Monographs* **82**(4). DOI: 10.1890/11-2164.1.

Vicente-Serrano SMM, Zabalza-Martínez J, Borràs G, López-Moreno JII, Pla E, Pascual D, Savé R, Biel C, Funes I, Azorin-Molina C, Sanchez-Lorenzo A, Martín-Hernández N, Peña-Gallardo M, Alonso-González E, Tomas-Burguera M, El Kenawy A. 2017. Extreme hydrological events and the influence of reservoirs in a highly regulated river basin of northeastern Spain. *Journal of Hydrology: Regional Studies* **12**: 13–32. DOI: 10.1016/j.ejrh.2017.01.004.

White D, Richman M, Yarnal B. 1991. Climate regionalization and rotation of principal components. *International Journal of Climatology*. John Wiley & Sons, Ltd **11**(1): 1–25. DOI: 10.1002/joc.3370110102.

Wilhite DA, Pulwarty RS. 2017. Drought as Hazard: Understanding the Natural and Social Context. *Drought and Water Crises: Integrating Science, Management, and Policy*, 3–22.

WMO. 2012. Standardized Precipitation Index User Guide. .

Yang Y, Zhang S, McVicar TR, Beck HE, Zhang Y, Liu B. 2018. Disconnection Between Trends of Atmospheric Drying and Continental Runoff. *Water Resources Research* **54**(7): 4700–4713. DOI: 10.1029/2018WR022593.

Zahradníček P, Trnka M, Brázdil R, Možný M, Štěpánek P, Hlavinka P, Žalud Z, Malý A, Semerádová D, Dobrovolný P, Dubrovský M, Řezníčková L. 2015. The extreme drought episode of August 2011-May 2012 in the Czech Republic. *International*

Journal of Climatology, 3335–3352.

Zhang Q, Ficklin DL, Manzoni S, Wang L, Way D, Phillips RP, Novick KA. 2019. Response of ecosystem intrinsic water use efficiency and gross primary productivity to rising vapor pressure deficit. *Environmental Research Letters*.

888 Table 1: Percentage of series showing positive and negative SPI trends at seasonal (SPI-
889 3) and annual (SPI-12) scales during the periods 1851-2018, 1861-2018 and 1871-2018.
890

891 Table2: Percentage of stations showing positive and negative trends in drought duration
892 and magnitude obtained from SPI-3- and SPI-12 series for the periods 1851-2018, 1861
893 -2018 and 1871 to 2018.

894 Table 3: Trends in the total area (%) impacted by different drought categories during the
895 period 1851-2018. Percentage change is expressed for the whole study period.
896 Significant at $p < 0.05$.
897

Table 1: Percentage of series showing positive and negative SPI trends at seasonal (SPI-3) and annual (SPI-12) scales during the periods 1851-2018, 1861-2018 and 1871-2018.

	Negative ($p < 0.05$)	Negative ($p > 0.05$)	Positive ($p > 0.05$)	Positive ($p < 0.05$)
Winter (1851)	0.0	8.7	47.0	44.3
Winter (1861)	1.2	15.2	53.8	29.8
Winter (1871)	1.0	15.6	51.3	32.2
Spring (1851)	4.4	25.4	56.1	14.0
Spring (1861)	5.8	31.0	45.6	17.5
Spring (1871)	9.5	30.2	46.7	13.6
Summer (1851)	12.2	67.0	20.9	0.0
Summer (1861)	8.8	61.4	29.2	0.6
Summer (1871)	16.6	61.8	21.6	0.0
Autumn (1851)	3.5	38.3	47.8	10.4
Autumn (1861)	2.3	48.5	46.8	2.3
Autumn (1871)	4.5	54.3	37.7	3.5
Annual (1851)	6.1	19.1	40.0	34.8
Annual (1861)	7.6	26.9	41.5	24.0
Annual (1871)	9.0	35.2	34.7	21.1

Table2: Percentage of stations showing positive and negative trends in drought duration and magnitude obtained from SPI-3- and SPI-12 series for the periods 1851-2018, 1861-2018 and 1871 to 2018.

	Negative ($p < 0.05$)	Negative ($p > 0.05$)	Positive ($p > 0.05$)	Positive ($p < 0.05$)
Magnitude 3 months (1851)	13.0	58.3	22.6	6.1
Magnitude 3 months (1861)	11.1	48.0	35.7	5.3
Magnitude 3 months (1871)	10.6	42.2	36.2	11.1
Duration 3 months (1851)	11.3	63.5	19.1	6.1
Duration 3 months (1861)	11.7	48.0	34.5	5.8
Duration 3 months (1871)	9.5	43.7	38.7	8.0
Magnitude 12 months (1851)	0.0	75.7	24.3	0.0
Magnitude 12 months (1861)	0.6	63.7	35.7	0.0
Magnitude 12 months (1871)	1.0	54.3	44.2	0.5
Duration 12 months (1851)	1.7	72.2	26.1	0.0
Duration 12 months (1861)	0.6	62.0	37.4	0.0
Duration 12 months (1871)	2.5	52.8	43.7	1.0

Table 3: Trends in the total area (%) impacted by different drought categories during the period 1851-2018. Percentage change is expressed for the whole study period. Significant at $p < 0.05$.

	Winter	Spring	Summer	Autumn	Annual
Mild (whole Europe)	-9.2	3.0	6.4	2.5	0.9
Moderate (whole Europe)	-5.5	1.5	4.8	2.9	1.5
Severe (whole Europe)	**-3.6***	1.4	2.8	1.7	1.4
Mild (Northern Europe)	**-12.6***	-0.5	6.9	0.3	-4.0
Moderate (Northern Europe)	**-9.0***	-0.3	5.3	1.1	-3.5
Severe (Northern Europe)	**-6.3***	0.0	3.0	0.3	-0.8
Mild (Southern Europe)	-3.9	5.8	4.6	4.1	1.8
Moderate (Southern Europe)	-0.8	3.1	3.2	4.0	1.0
Severe (Southern Europe)	-0.1	2.4	2.1	2.8	1.2

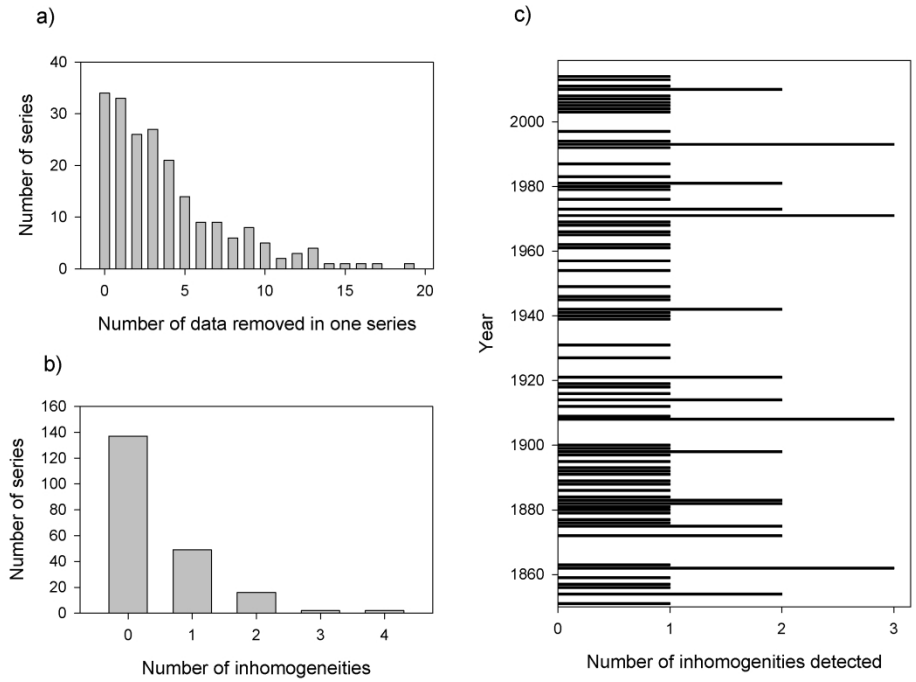

Figure 1: a) Frequency of the number of cases (months) removed from each series after quality control checks, b) the number of inhomogeneities detected in the series, and c) distribution of detected inhomogeneities as a function of time.

807x645mm (96 x 96 DPI)

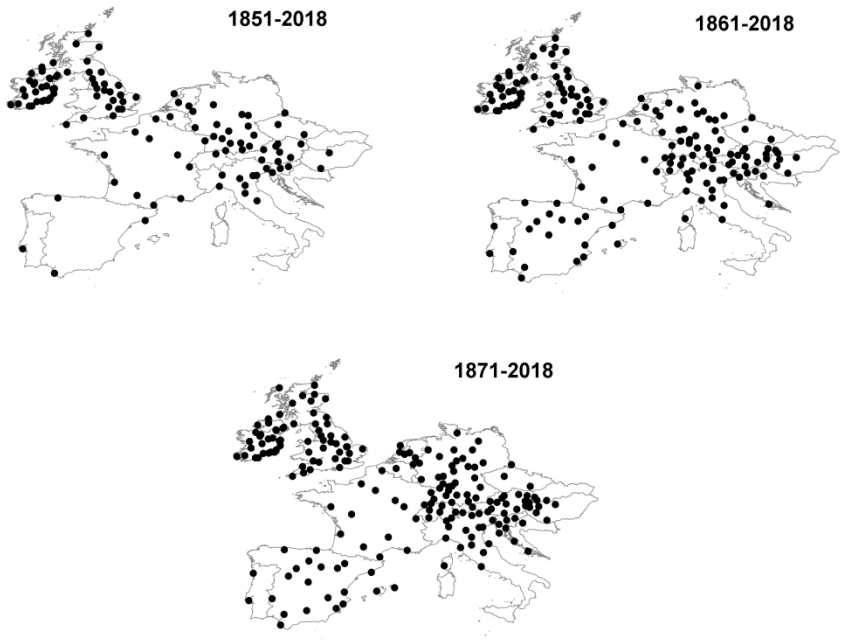

Figure 2. Spatial distribution of the available precipitation stations employed for different analysis periods.

269x195mm (300 x 300 DPI)

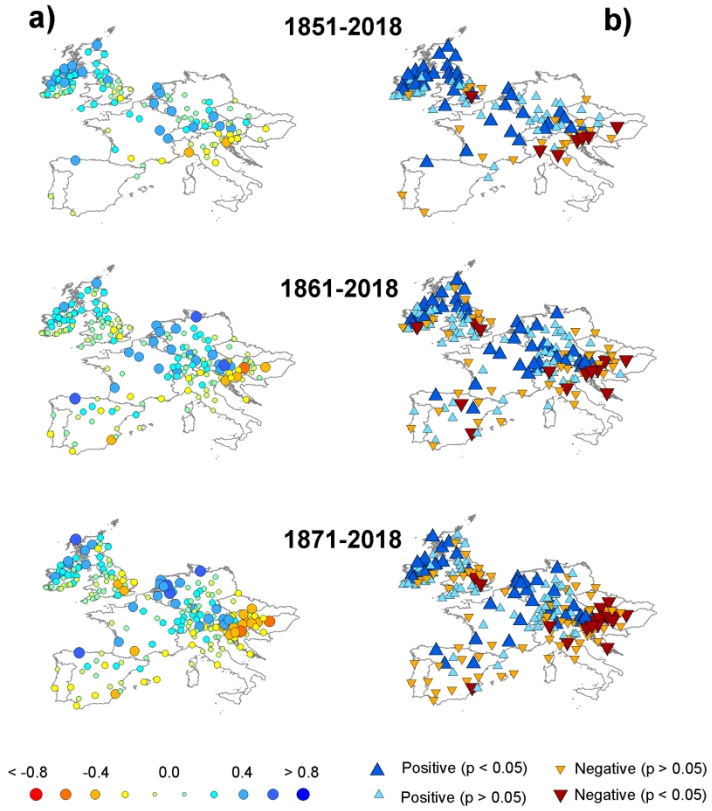

Figure 3. Spatial distribution of (a) the magnitude of change in annual SPI series (December SPI-12) and (b) their statistical significance. The magnitude of change is expressed in z units/decade.

226x209mm (300 x 300 DPI)

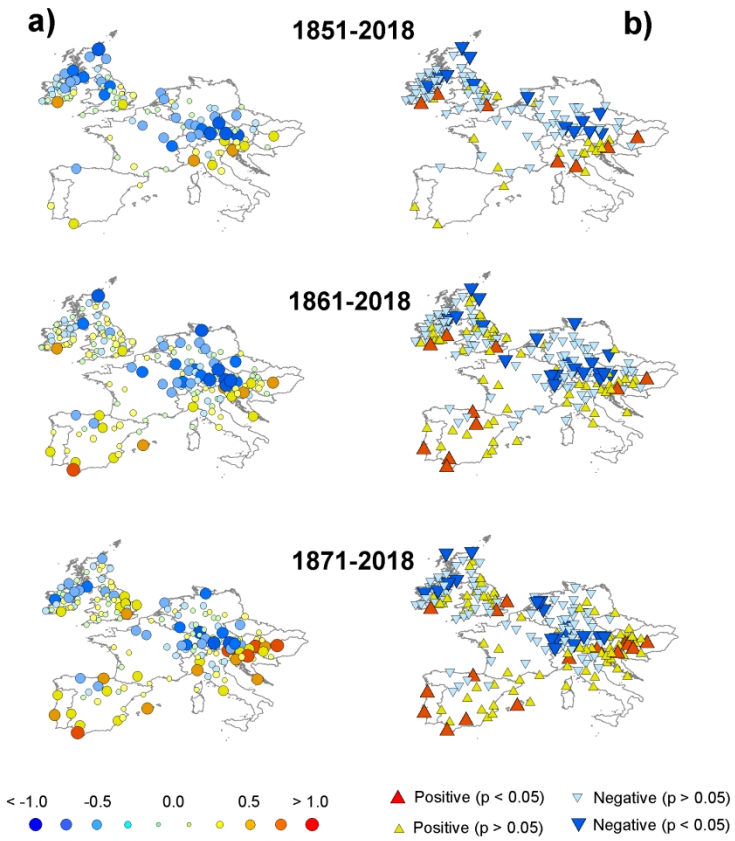

Figure 4. Spatial distribution of changes in the duration of drought events based on SPI-3 series (a) and (b) their statistical significance. Changes are expressed in months/decade.

218x209mm (300 x 300 DPI)

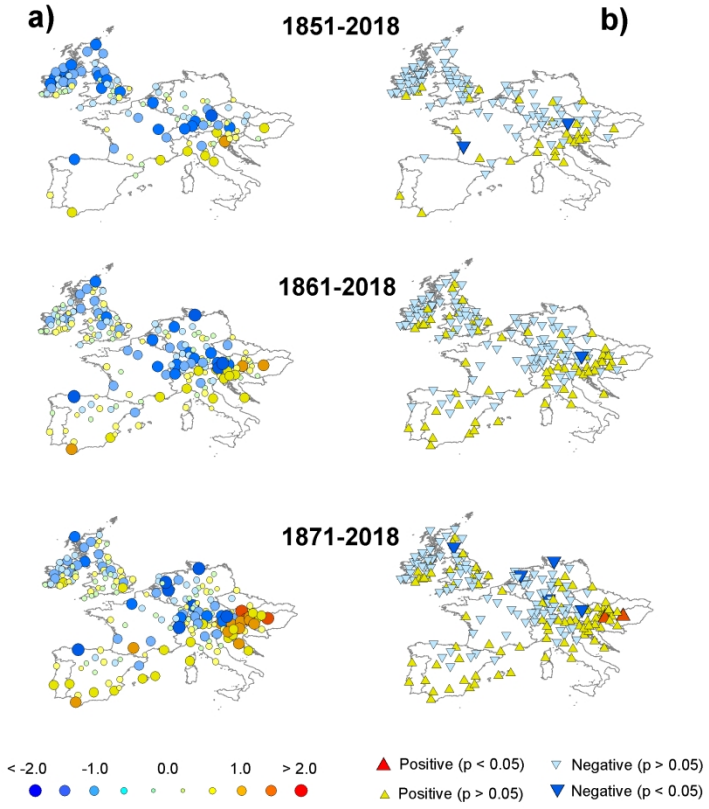

Figure 5. Spatial distribution of changes in the duration of drought events based on SPI-12 series (a) and (b) their statistical significance. Changes are expressed in months/decade.

227x209mm (300 x 300 DPI)

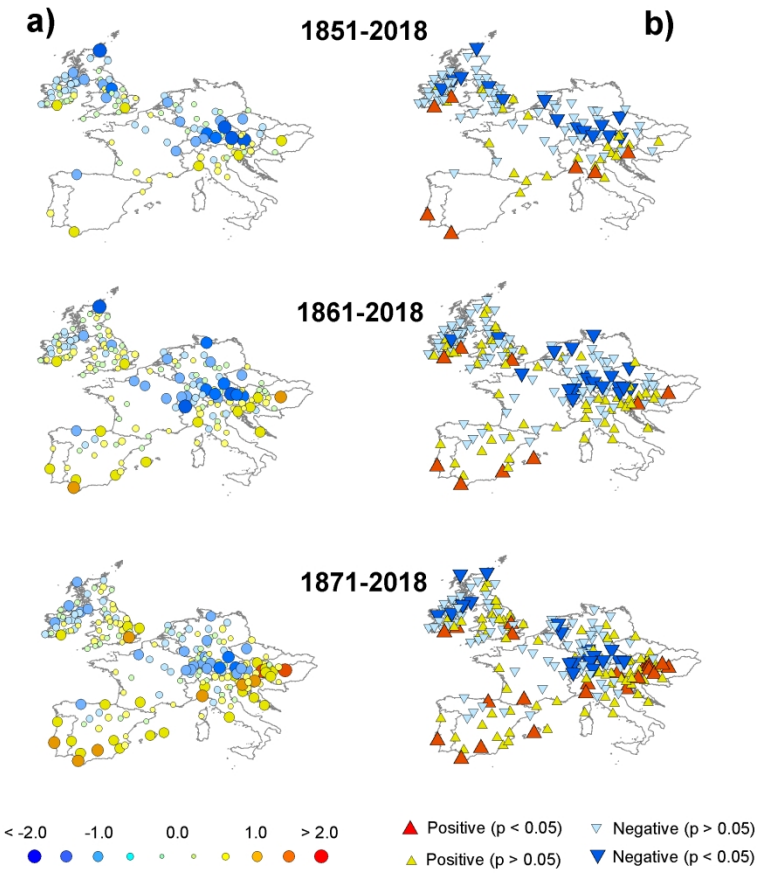

Figure 6. Spatial distribution of changes in the magnitude of drought events based on SPI-3 series (a) and (b) their statistical significance. Changes are expressed in cumulative z-units/decade.

210x209mm (300 x 300 DPI)

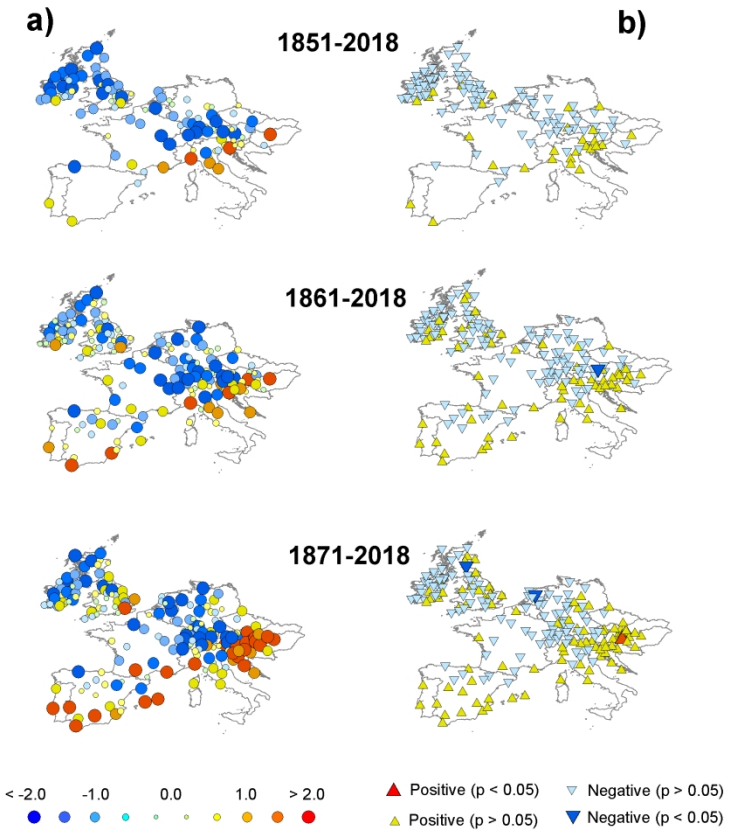

Figure 7. Spatial distribution of changes in the magnitude of drought events based on the SPI-12 series (a) and (b) their statistical significance. Changes are expressed in cummulative z-units/decade.

220x209mm (300 x 300 DPI)

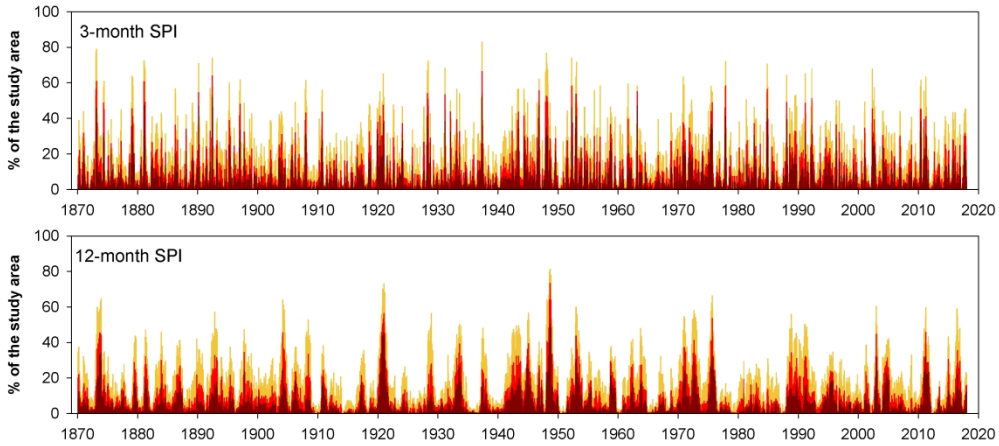

Figure 8: Evolution of the European land area impacted by mild (orange), moderate (red) and severe droughts (dark read) from 1871 to 2018.

278x130mm (300 x 300 DPI)

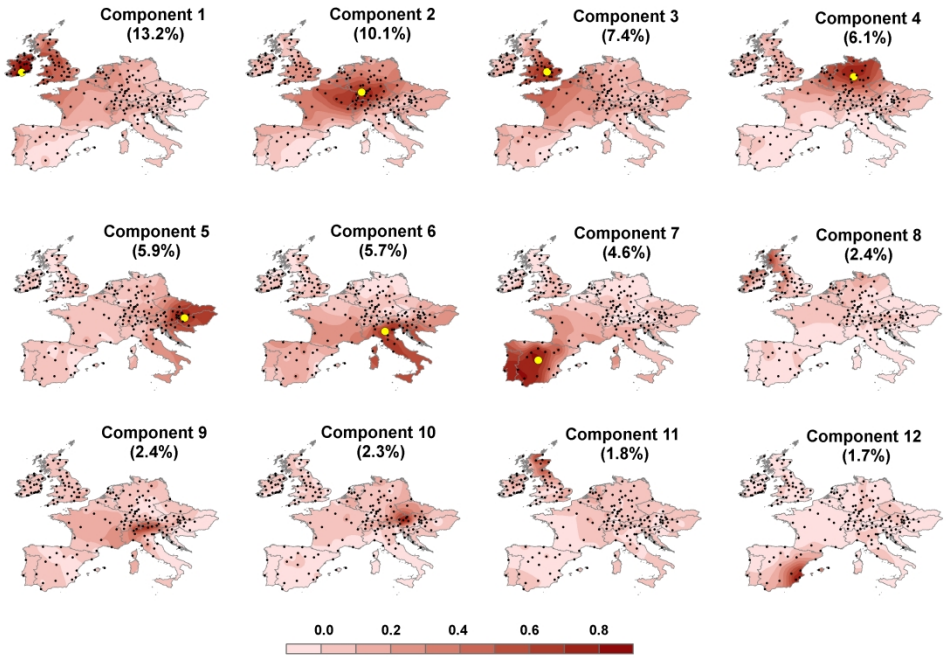

Figure 9: Spatial distribution of the loadings from PCA using SPI-12 series for the period 1871-2018. Components 1 to 12 are shown. The proportion of variance explained by each component is also included. Yellow points represent the location of the most representative meteorological station.

296x210mm (300 x 300 DPI)

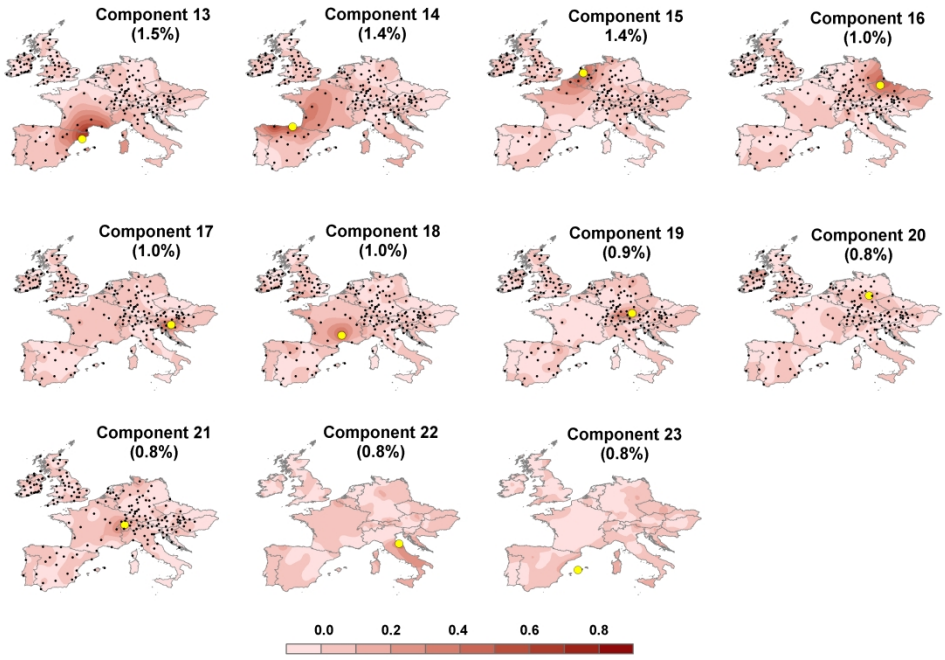

Figure 9 cont.: Spatial distribution of the loadings from PCA using SPI-12 series for the period 1871-2018. Components 13 to 23 are shown. The proportion of variance explained by each component is also included. Yellow points represent the location of the most representative meteorological station.

296x210mm (300 x 300 DPI)

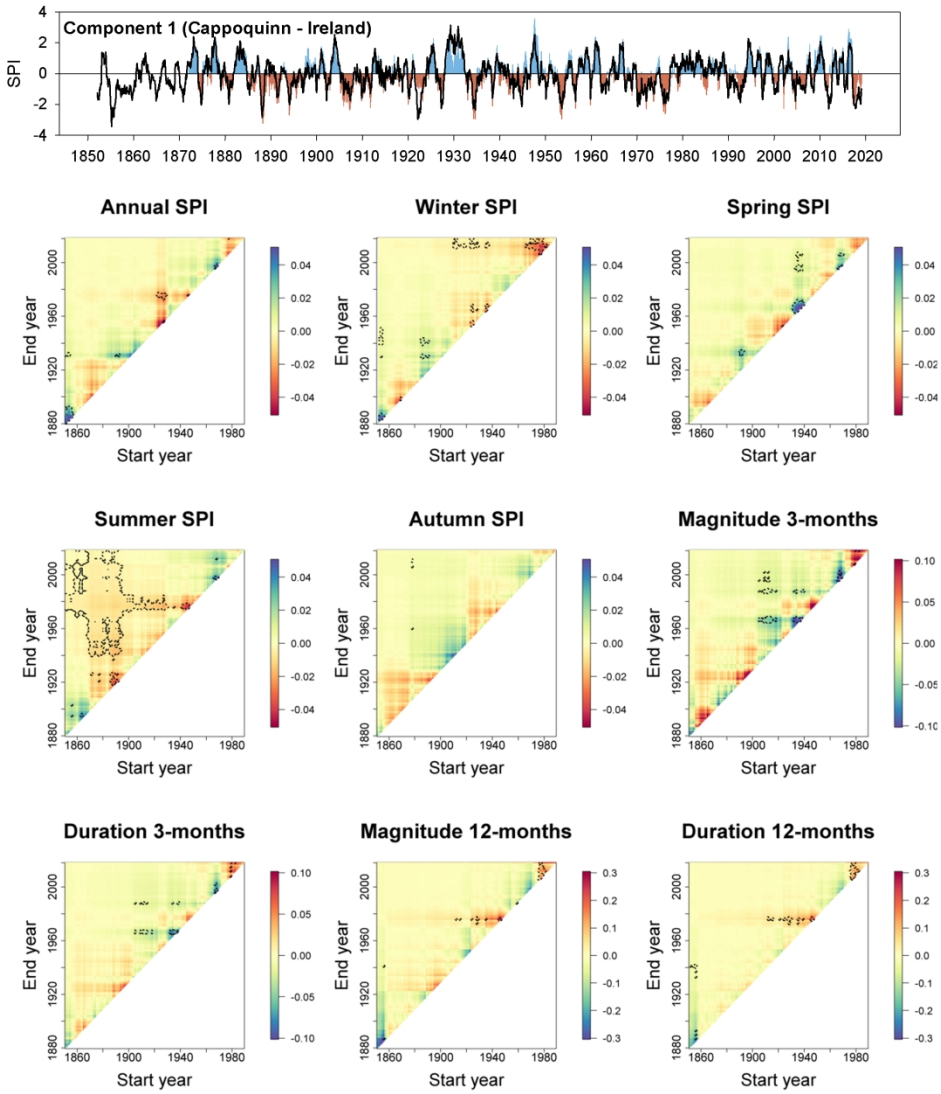

Figure 10: Temporal evolution of the SPI-12 series of component 1 in color and the series of the most representative station (black line). The correlation between the series of the component and the series of the station is r = 0.85. Also shown are heat maps of 30-year running trends in annual and seasonal SPI and 3- and 12-month SPI drought duration and magnitude for the station of Cappoquin (Ireland). X and Y-axes indicate the start and end years, respectively, of the time slices for the running trend analysis. The scale indicates the magnitude of the trend based on the slope of the linear regression analysis. Dotted lines indicate periods with a significant trend ($p<0.05$).

645x807mm (96 x 96 DPI)

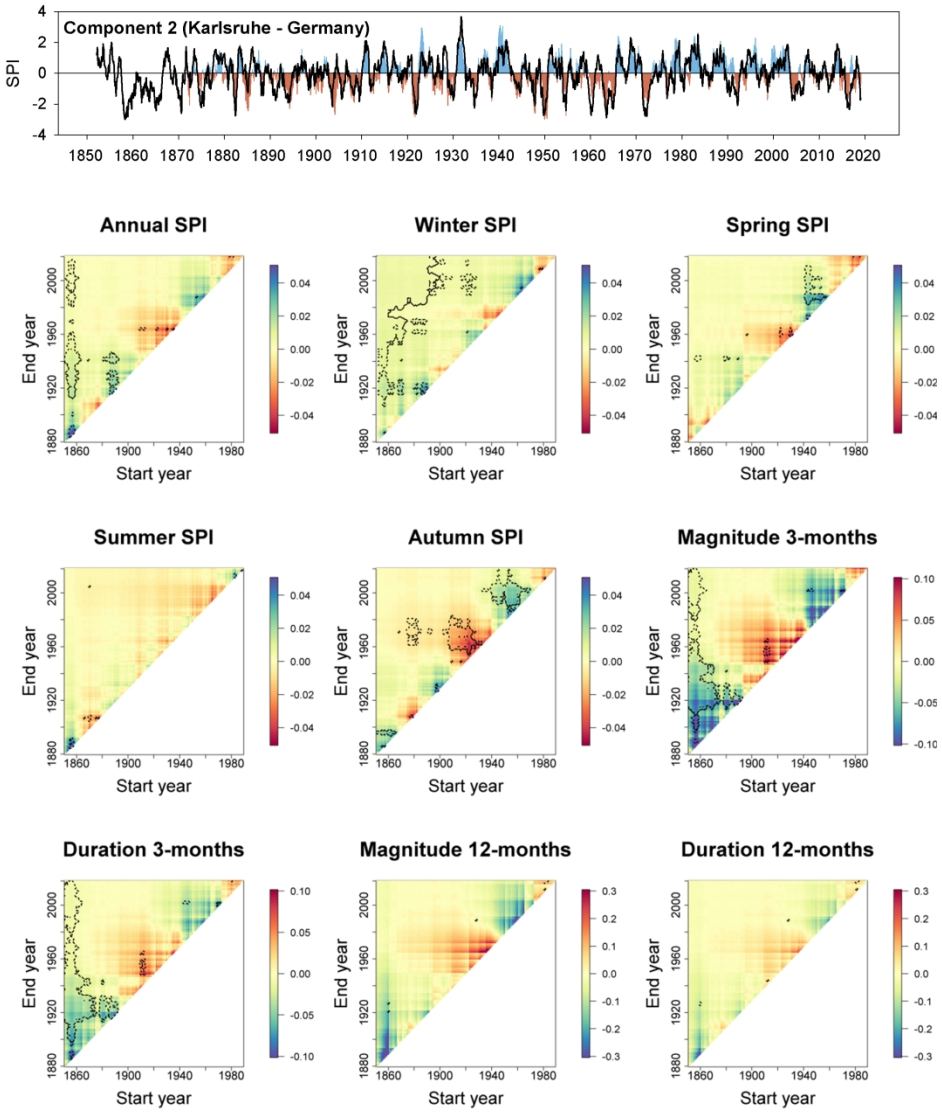

Figure 11: Temporal evolution of the SPI-12 series of component 2 in color and the series of the most representative station (black line). The correlation between the series of the component and the series of the station is r = 0.75. Also shown are heat maps of 30-year running trends in annual and seasonal SPI and 3- and 12-month SPI drought duration and magnitude for the station of Karlsruhe (Germany). X and Y-axes indicate the start and end years, respectively, of the time slices for the running trend analysis. The scale indicates the magnitude of the trend based on the slope of the linear regression analysis. Dotted lines indicate periods with a significant trend ($p<0.05$).

645x807mm (96 x 96 DPI)

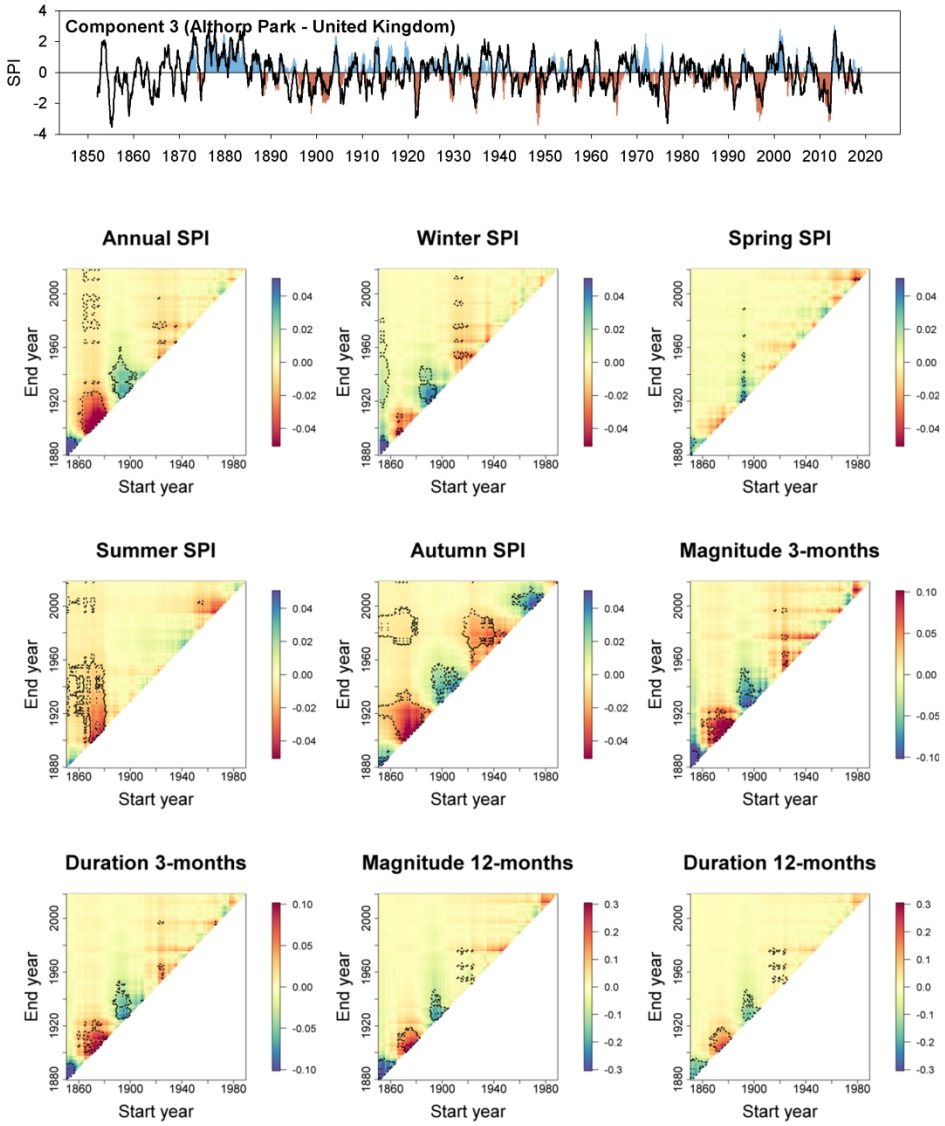

Figure 12: Temporal evolution of the SPI-12 series of component 3 in color and the series of the most representative station (black line). The correlation between the series of the component and the series of the station is r = 0.76. Also shown are heat maps of 30-year running trends in annual and seasonal SPI and 3- and 12-month SPI drought duration and magnitude for the station of Althorp Park (United Kingdom). X and Y-axes indicate the start and end years, respectively, of the time slices for the running trend analysis. The scale indicates the magnitude of the trend based on the slope of the linear regression analysis. Dotted lines indicate periods with a significant trend ($p<0.05$).

645x807mm (96 x 96 DPI)

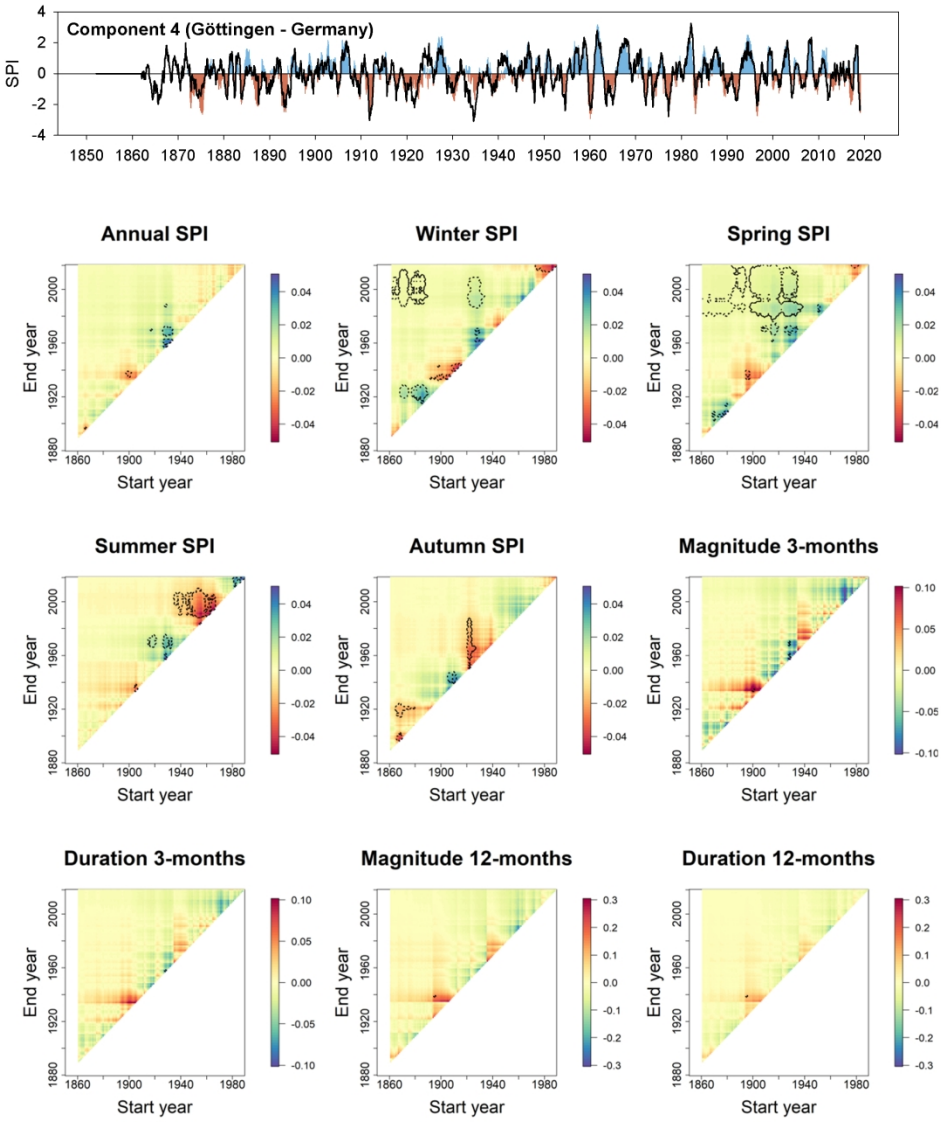

Figure 13: Temporal evolution of the SPI-12 series of component 4 in color and the series of the most representative station (black line). The correlation between the series of the component and the series of the station is r = 0.80. Also shown are heat maps of 30-year running trends in annual and seasonal SPI and 3- and 12-month SPI drought duration and magnitude for the station of Göttingen (Germany). X and Y-axes indicate the start and end years, respectively, of the time slices for the running trend analysis. The scale indicates the magnitude of the trend based on the slope of the linear regression analysis. Dotted lines indicate periods with a significant trend ($p<0.05$).

645x807mm (96 x 96 DPI)

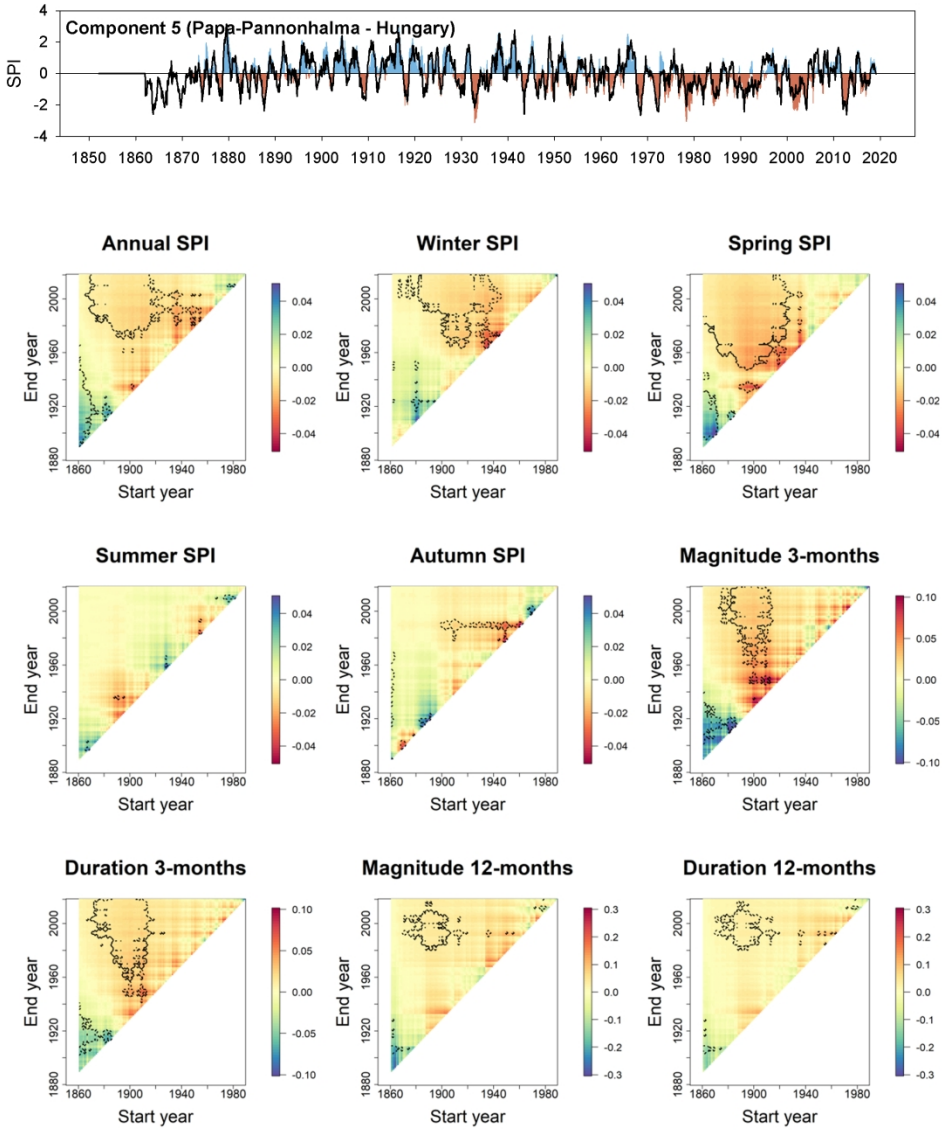

Figure 14: Temporal evolution of the SPI-12 series of component 5 in color and the series of the most representative station (black line). The correlation between the series of the component and the series of the station is r = 0.84. Also shown are heat maps of 30-year running trends in annual and seasonal SPI and 3- and 12-month SPI drought duration and magnitude for the station of Papa-Pannonhalma (Hungary). X and Y-axes indicate the start and end years, respectively, of the time slices for the running trend analysis. The scale indicates the magnitude of the trend based on the slope of the linear regression analysis. Dotted lines indicate periods with a significant trend ($p<0.05$).

645x807mm (96 x 96 DPI)

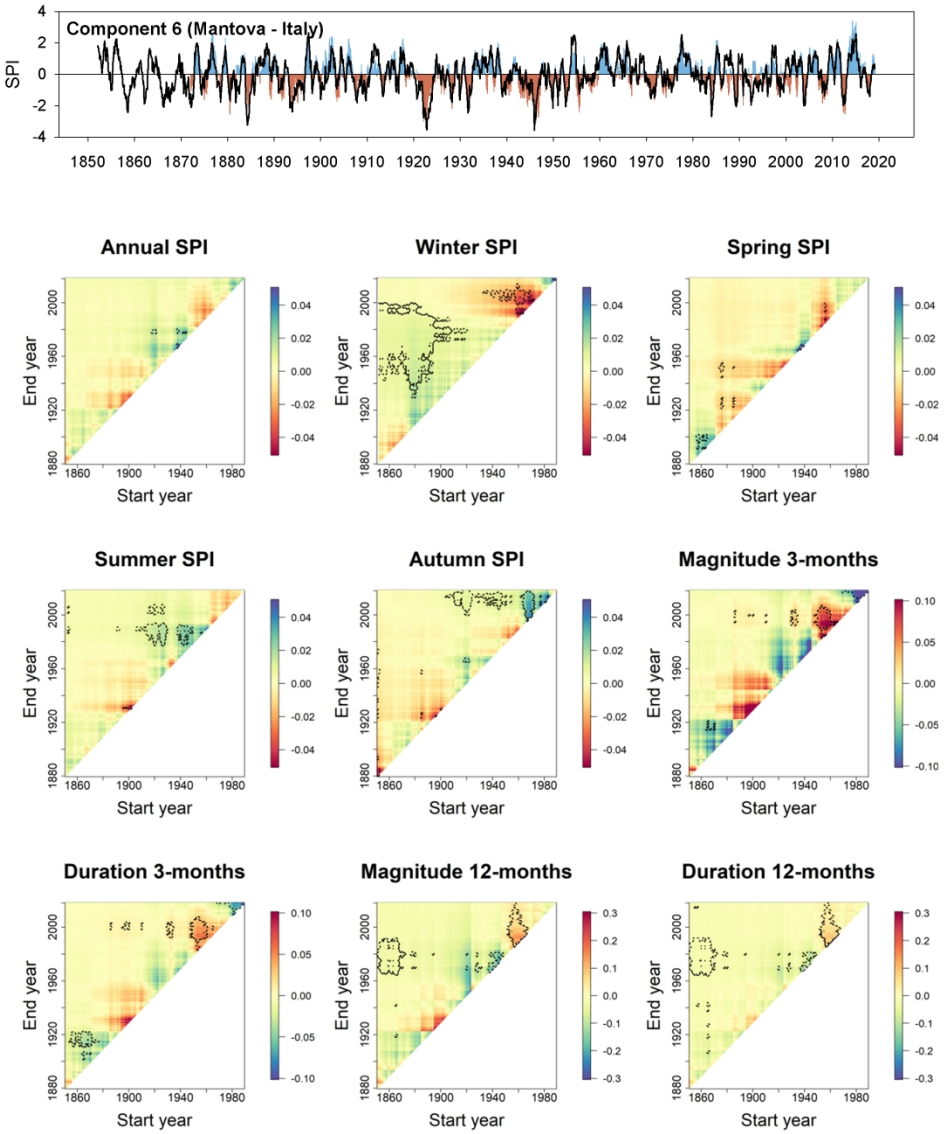

Figure 15: Temporal evolution of the SPI-12 series of component 6 in color and the series of the most representative station (black line). The correlation between the series of the component and the series of the station is r = 0.78. Also shown are heat maps of 30-year running trends in annual and seasonal SPI and 3- and 12-month SPI drought duration and magnitude for the station of Mantova (Italy). X and Y-axes indicate the start and end years, respectively, of the time slices for the running trend analysis. The scale indicates the magnitude of the trend based on the slope of the linear regression analysis. Dotted lines indicate periods with a significant trend ($p<0.05$).

645x807mm (96 x 96 DPI)

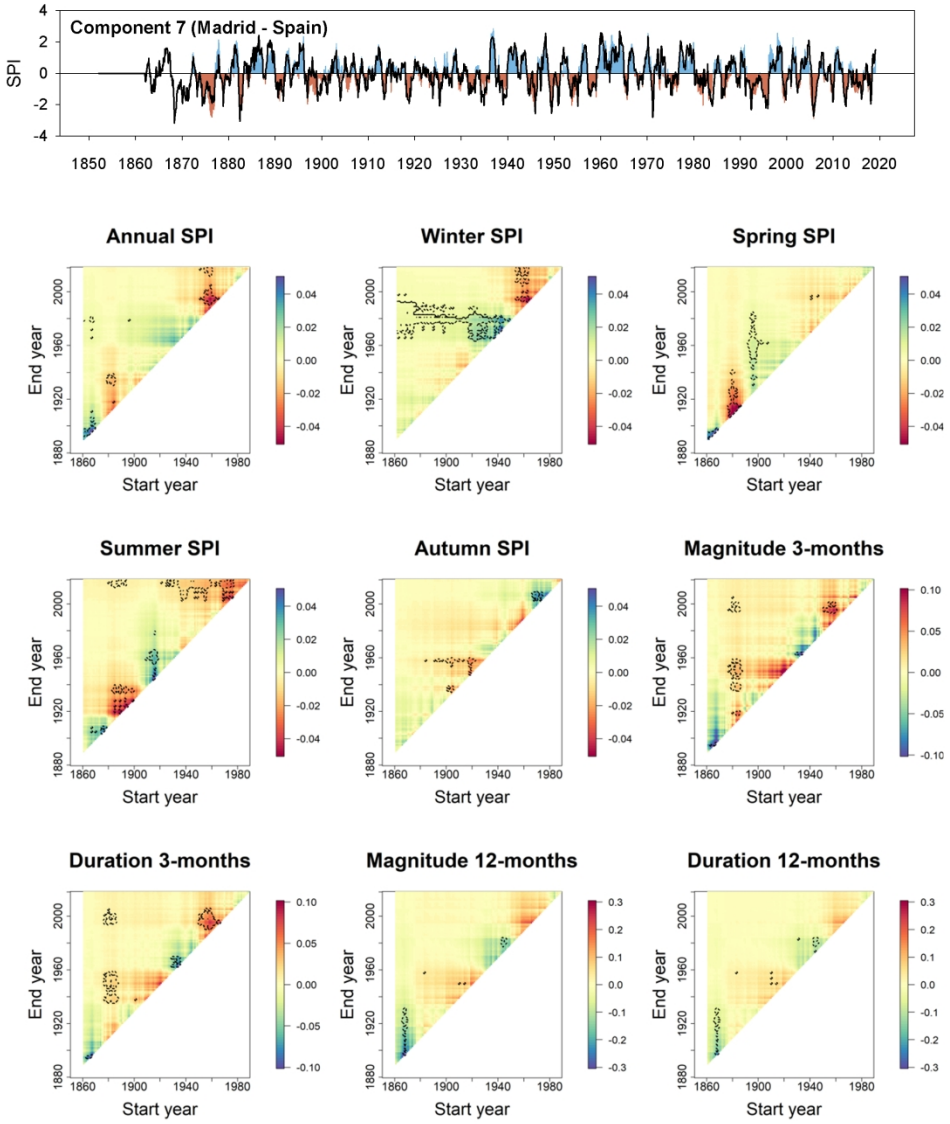

Figure 16: Temporal evolution of the SPI-12 series of component 7 in color and the series of the most representative station (black line). The correlation between the series of the component and the series of the station is r = 0.86. Also shown are heat maps of 30-year running trends in annual and seasonal SPI and 3- and 12-month SPI drought duration and magnitude for the station of Madrid (Spain). X and Y-axes indicate the start and end years, respectively, of the time slices for the running trend analysis. The scale indicates the magnitude of the trend based on the slope of the linear regression analysis. Dotted lines indicate periods with a significant trend ($p<0.05$).

645x807mm (96 x 96 DPI)

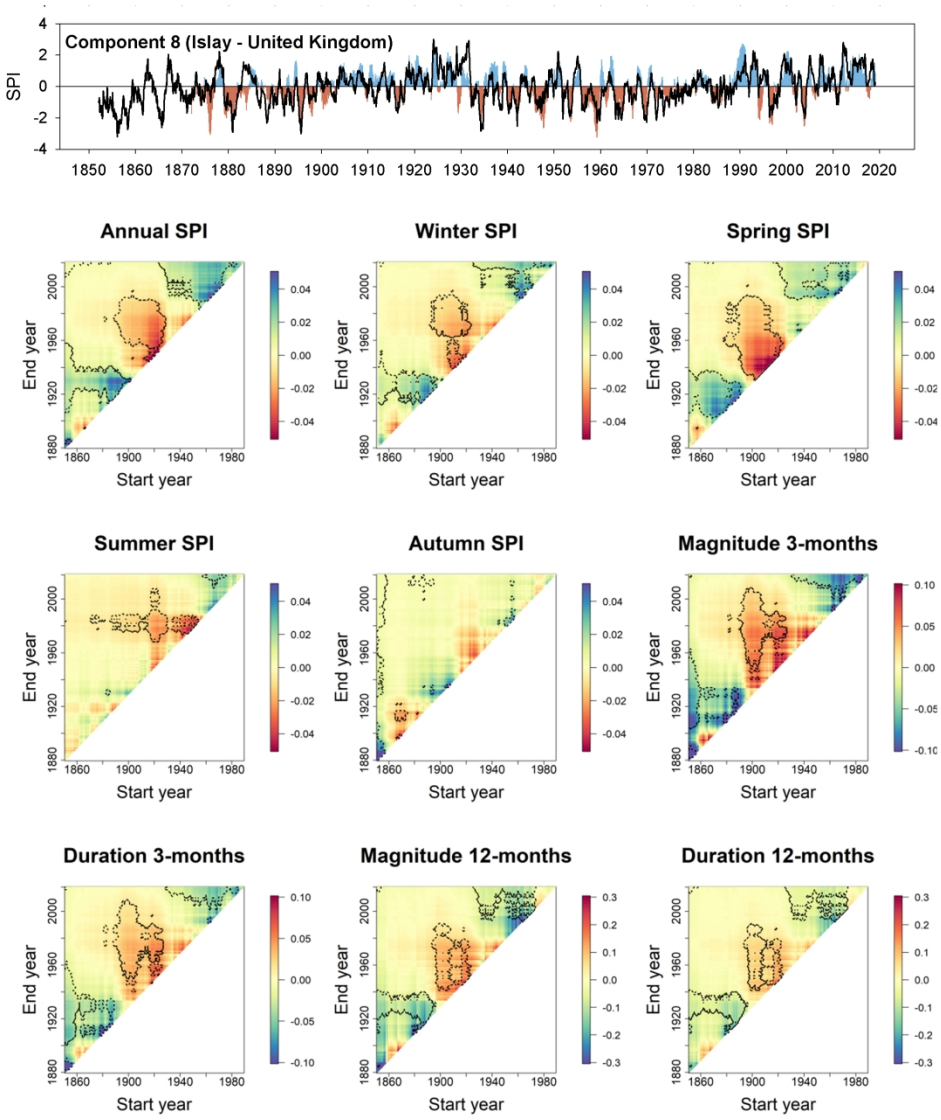

Figure 17: Temporal evolution of the SPI-12 series of component 8 in color and the series of the most representative station (black line). The correlation between the series of the component and the series of the station is r = 0.70. Also shown are heat maps of 30-year running trends in annual and seasonal SPI and 3- and 12-month SPI drought duration and magnitude for the station of Islay (United Kingdom). X and Y-axes indicate the start and end years, respectively, of the time slices for the running trend analysis. The scale indicates the magnitude of the trend based on the slope of the linear regression analysis. Dotted lines indicate periods with a significant trend ($p<0.05$).

645x807mm (96 x 96 DPI)

Long-term variability and trends in meteorological droughts in Europe (1851-2018)

Vicente-Serrano, S.M.[1], Domínguez-Castro, F.[2], Murphy, C.[3], Hannaford, J.[3,4], Reig, F.[1], Peña-Angulo, D.[1], Tramblay, Y.[5], Trigo, R.M.[6], Macdonald, N.[7], Luna, M.Y.[8], McCarthy, M.[9], Van der Schrier, G.[10], Turco, M.[11], Camuffo, D.[12], Noguera, I.[1], El Kenawy, A.[13,14], García-Herrera, R.[15,16], Becherini, F.[12,17], della Valle, A.[12]

[1]Instituto Pirenaico de Ecología, Consejo Superior de Investigaciones Científicas (IPE–CSIC), Zaragoza, Spain,
[2]Aragonese Agency for Research and Development Researcher, Department of Geography, University of Zaragoza, Zaragoza, Spain
[3]Irish Climate Analysis and Research UnitS (ICARUS), Department of Geography, Maynooth University, Maynooth, Ireland,
[4]Centre for Ecology and Hydrology, Wallingford, United Kingdom,
[5]HSM (Univ. Montpellier, CNRS, IRD), Montpellier, France
[6]Instituto Dom Luiz (IDL), Faculdade de Ciências, Universidade de Lisboa, Lisboa, Portugal
[7]School of Environmental Sciences, University of Liverpool, Liverpool
[8]Agencia Estatal de Meteorología (AEMET), Madrid, Spain
[9]Met Office National Climate Information Centre, Exeter, United Kingdom,
[10]Royal Netherlands Meteorological Institute (KNMI), De Bilt, Netherlands
[11]Regional Atmospheric Modeling Group, Department of Physics, University of Murcia, Spain
[12]Institute of Atmospheric Sciences and Climate (CNR-ISAC), Padova, Italy
[13]Department of Geography, Mansoura University, Mansoura, Egypt
[14]Department of Geography, Sultan Qaboos University, Al Khoud, Muscat, Oman
[15] Departamento de Ciencias de la Tierra y Astrofísica, Facultad de Ciencias Físicas, Universidad Complutense de Madrid, Madrid, Spain
[16] Instituto de Geociencias (CIS-UCM) Madrid, Spain
[17] Institute of Polar Sciences (CNR-ISP), Venice, Italy

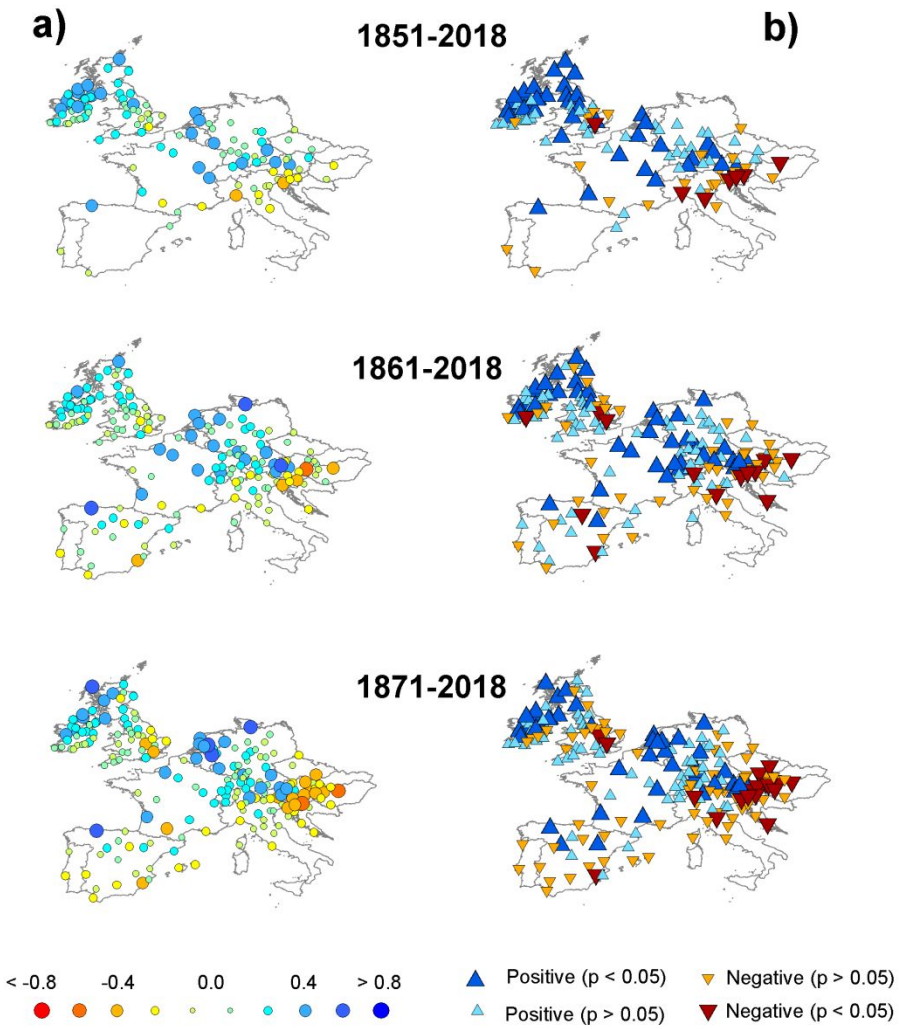

Spatial distribution of (a) the magnitude of change in annual SPI series (December SPI-12) and (b) their statistical significance. The magnitude of change is expressed in z units/decade.

Supplementary material for:

Long-term variability and trends in meteorological droughts in Western Europe (1851-2018)

Vicente-Serrano, S.M.[1], Domínguez-Castro, F.[2], Murphy, C.[3], Hannaford, J.[3,4], Reig, F.[1], Peña-Angulo, D.[1], Tramblay, Y.[5], Trigo, R.M.[6], MacDonald, N.[7], Luna, M.Y.[8], McCarthy, M.[9], Van der Schrier, G.[10], Turco, M.[11], Camuffo, D.[12], Noguera, I.[1], García-Herrera, R.[13,14], Becherini, F.[12,15], della Valle, A.[12], Tomas-Burguera, M.[16], El Kenawy, A.[17,18]

[1]Instituto Pirenaico de Ecología, Consejo Superior de Investigaciones Científicas (IPE–CSIC), Zaragoza, Spain,
[2]Aragonese Agency for Research and Development Researcher, Department of Geography, University of Zaragoza, Zaragoza, Spain
[3]Irish Climate Analysis and Research UnitS (ICARUS), Department of Geography, Maynooth University, Maynooth, Ireland,
[4]Centre for Ecology and Hydrology, Wallingford, United Kingdom,
[5]HSM (Univ. Montpellier, CNRS, IRD), Montpellier, France
[6]Instituto Dom Luiz (IDL), Faculdade de Ciências, Universidade de Lisboa, Lisboa, Portugal
[7]School of Environmental Sciences, University of Liverpool, Liverpool
[8]Agencia Estatal de Meteorología (AEMET), Madrid, Spain
[9]Met Office National Climate Information Centre, Exeter, United Kingdom,
[10]Royal Netherlands Meteorological Institute (KNMI), De Bilt, Netherlands
[11]Regional Atmospheric Modeling Group, Department of Physics, University of Murcia, Spain
[12]Institute of Atmospheric Sciences and Climate (CNR-ISAC), Padova, Italy
[13] Departamento de Ciencias de la Tierra y Astrofísica, Facultad de Ciencias Físicas, Universidad Complutense de Madrid, Madrid, Spain
[14] Instituto de Geociencias (CIS-UCM) Madrid, Spain
[15] Institute of Polar Sciences (CNR-ISP), Venice, Italy
[16]Estación Experimental de Aula Dei, Consejo Superior de Investigaciones Científicas (EEAD–CSIC), Zaragoza, Spain.
[17]Department of Geography, Mansoura University, Mansoura, Egypt
[18]Department of Geography, Sultan Qaboos University, Al Khoud, Muscat, Oman

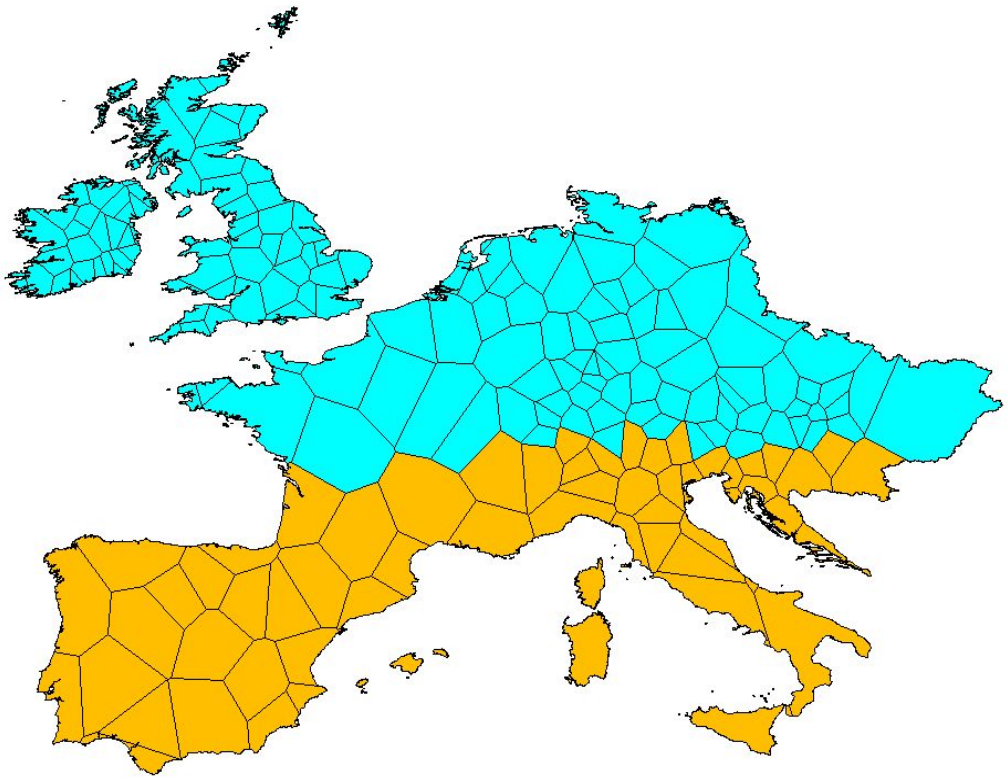

Supplementary Figure 1: Spatial distribution of the study domain according to the available meteorological stations by means of Thiessen polygons. Blue: central and North Europe area. Orange: South Europe area.

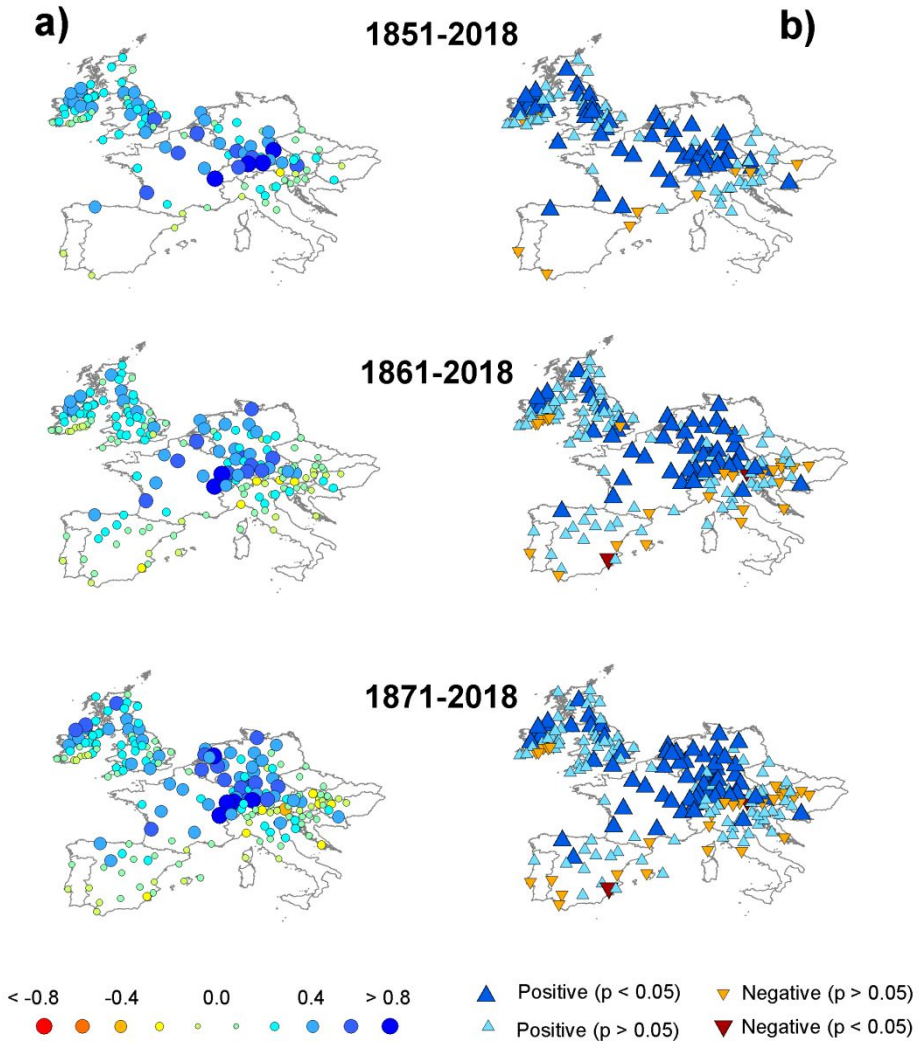

Supplementary Figure 2. Spatial distribution of the magnitude of change in winter SPI series (February SPI-3) (a) and (b) their statistical significance. Changes are expressed in z-units/decade.

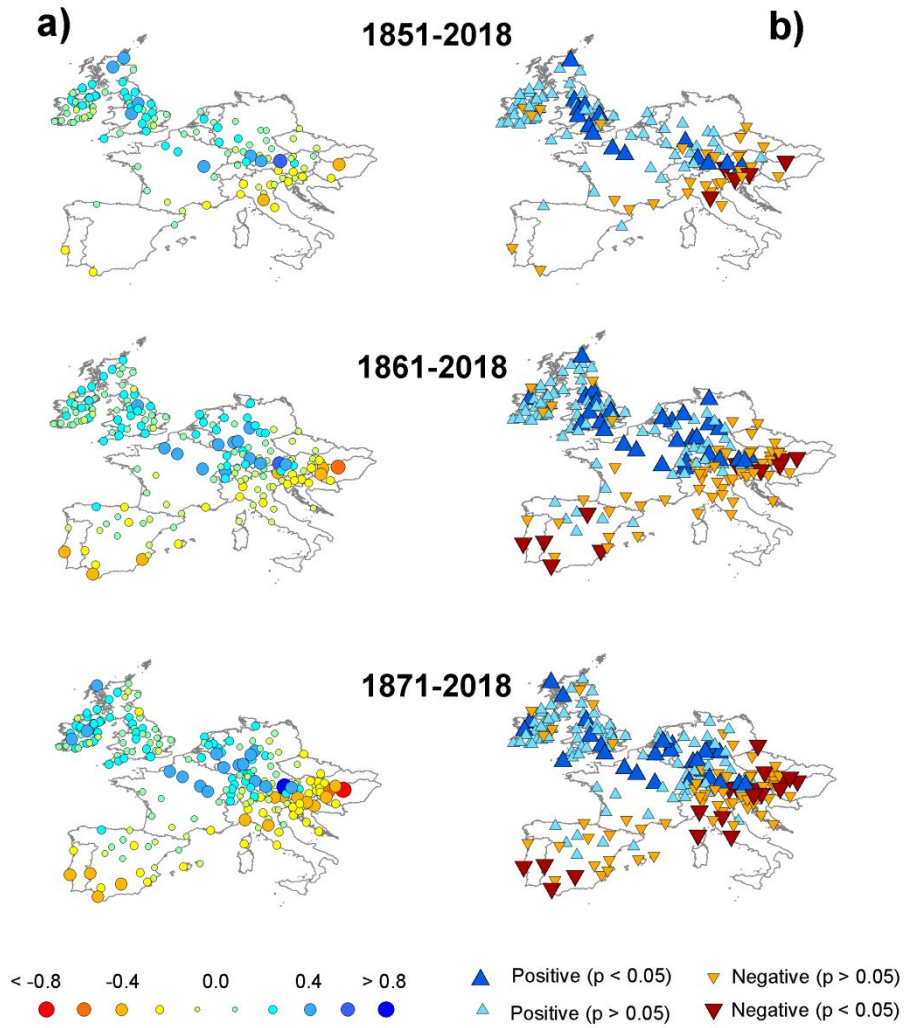

Supplementary Figure 3. Spatial distribution of the magnitude of change in spring SPI series (May SPI-3) (a) and (b) their statistical significance. Changes are expressed in z-units/decade.

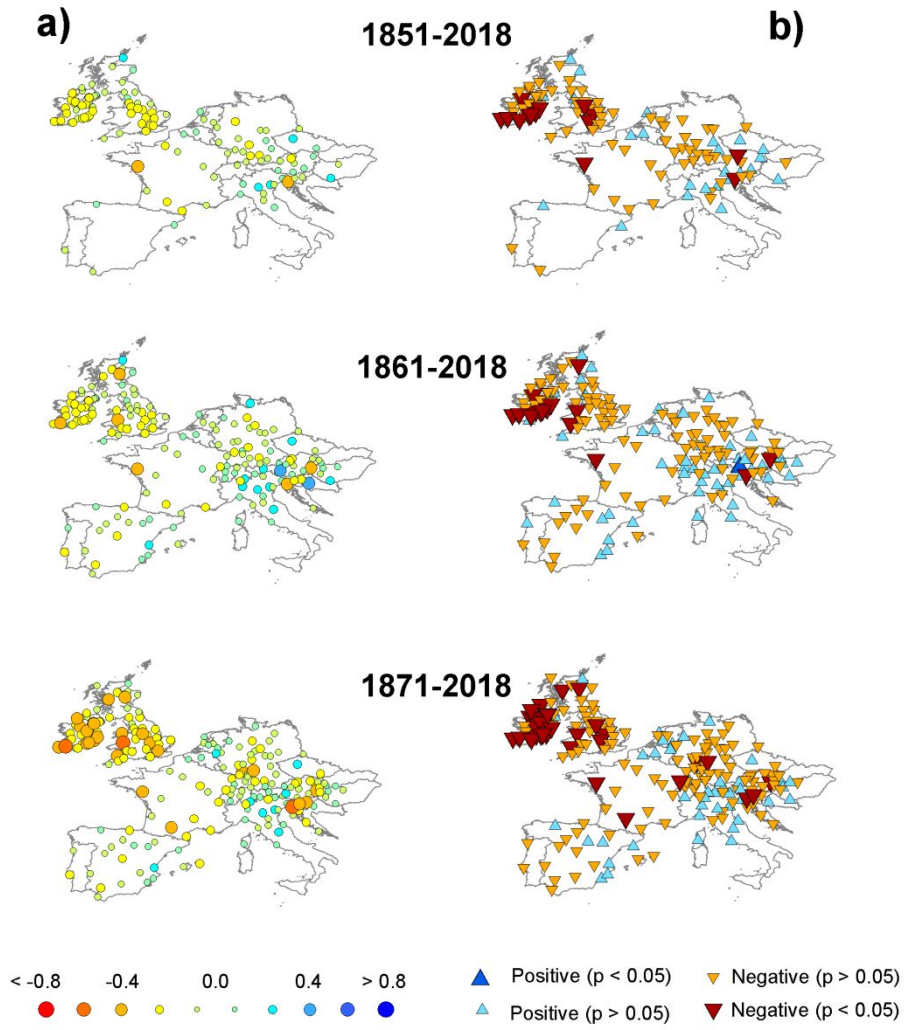

Supplementary Figure 4. Spatial distribution of the magnitude of change in summer SPI series (August SPI-3) (a) and (b) their statistical significance. Changes are expressed in z-units/decade.

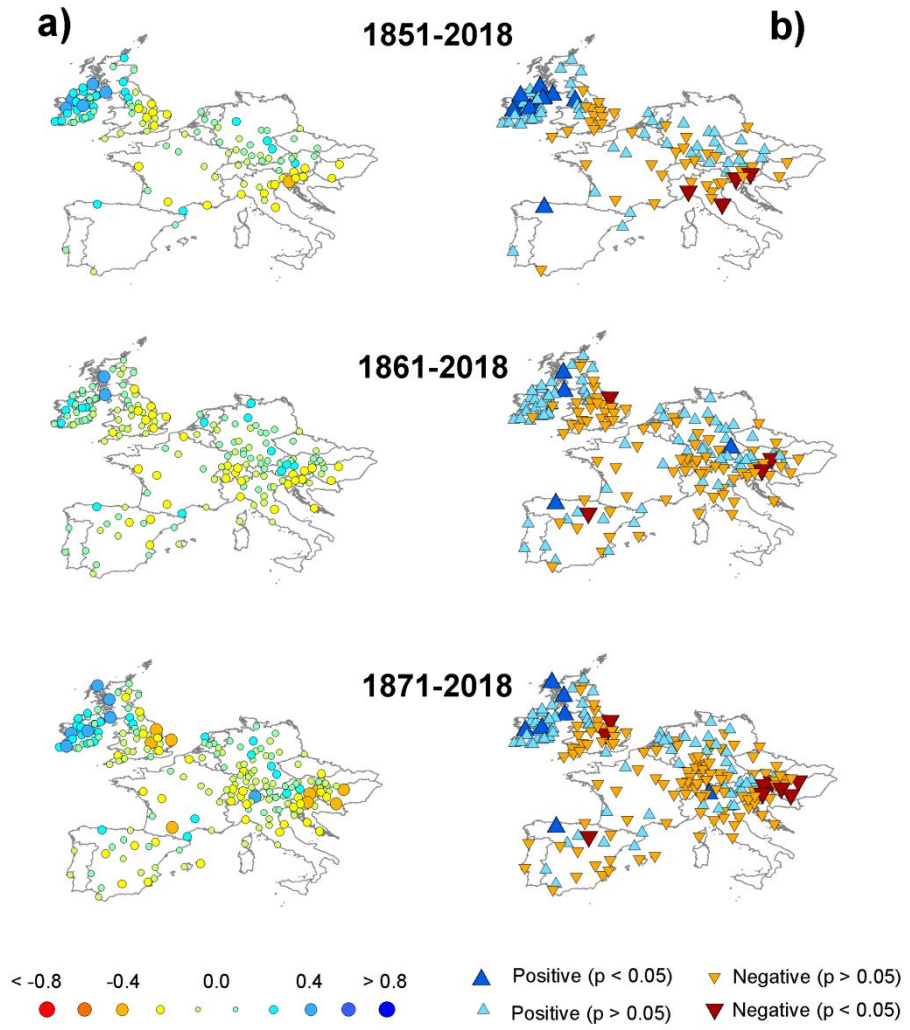

Supplementary Figure 5. Spatial distribution of the magnitude of change in autumn SPI series (November SPI-3) (a) and (b) their statistical significance. Changes are expressed in z-units/decade.

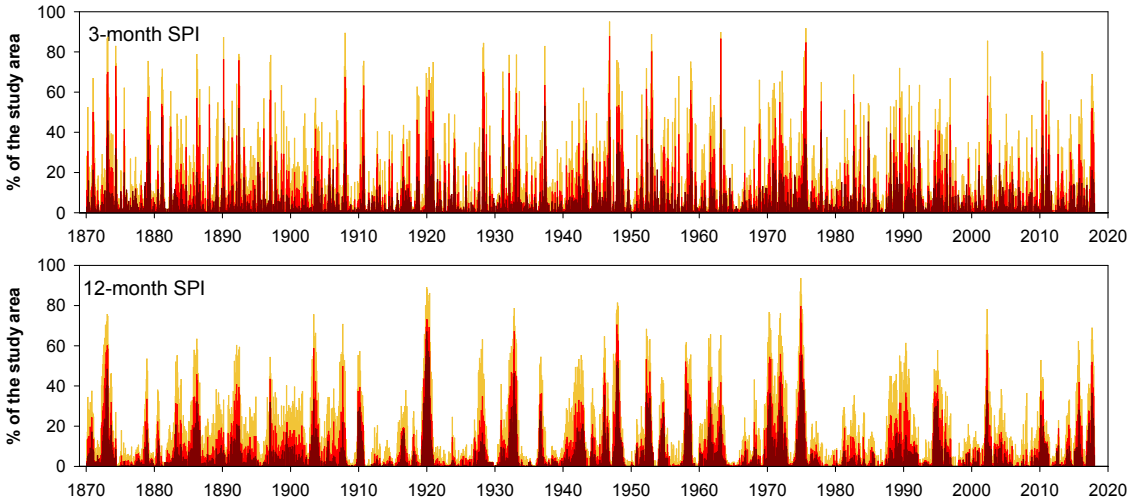

Supplementary Figure 6: Evolution of the total land area of Northern and Central Europe impacted by mild (orange), moderate (red) and severe droughts (dark read) in the study area.

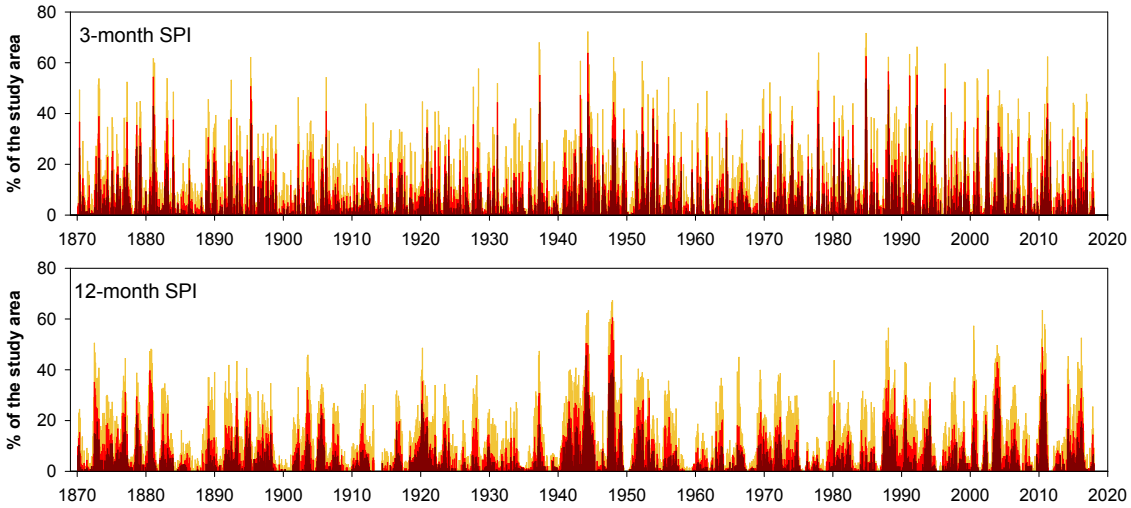

Supplementary Figure 7: Evolution of the total land area of Southern Europe impacted by mild (orange), moderate (red) and severe droughts (dark read) in the study area.

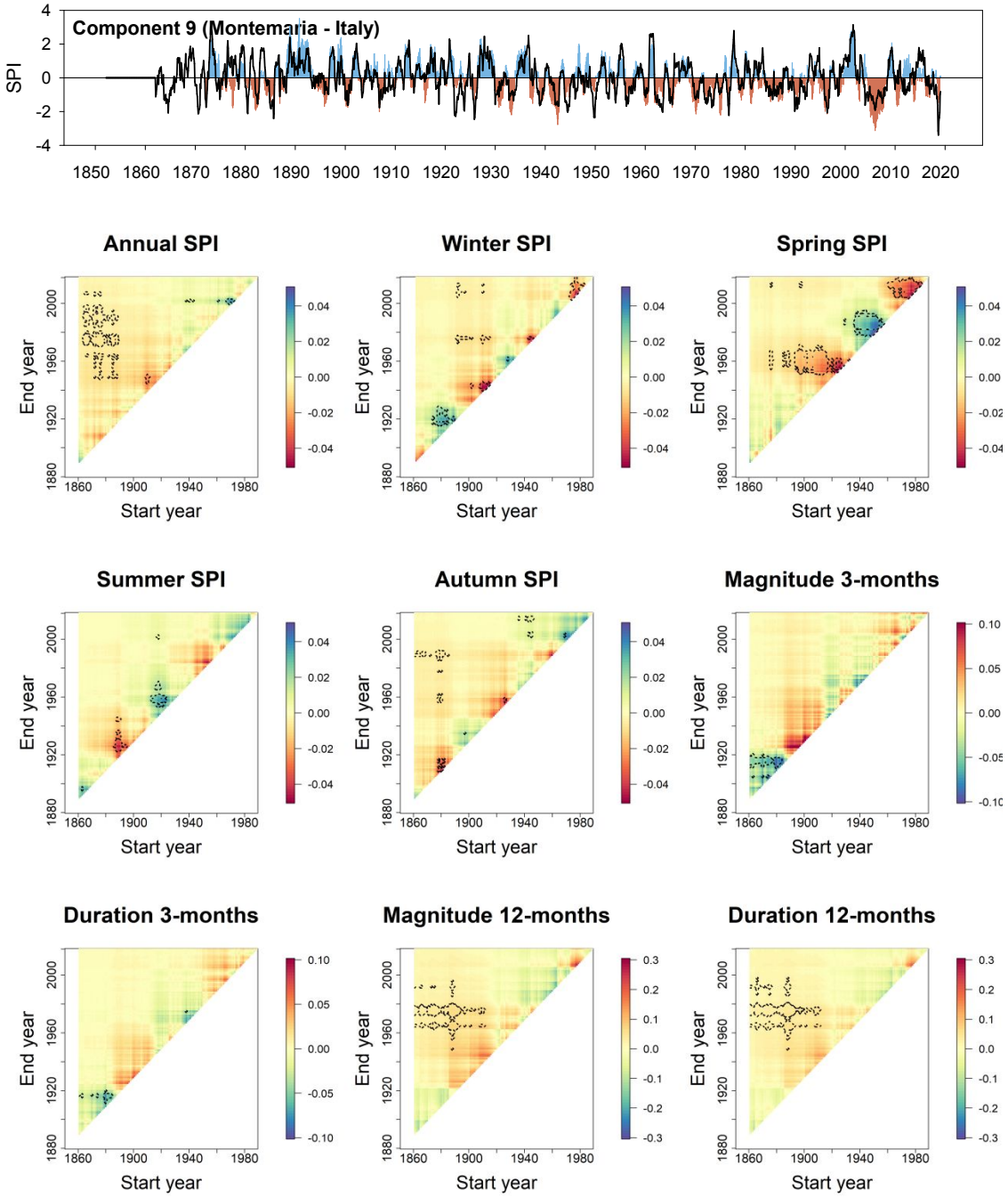

Supplementary Figure 8: Temporal evolution of the SPI-12 series of component 9 in color and the series of the most representative station (black line). The correlation between the series of the component and the series of the station is r = 0.71. Also shown are heat maps of 30-year running trends in annual and seasonal SPI and 3- and 12-month SPI drought duration and magnitude for the station of Montemaria (Italy). X and Y-axes indicate the start and end years, respectively, of the time slices for the running trend analysis. The scale indicates the magnitude of the trend based on the slope of the linear regression analysis. Dotted lines indicate periods with a significant trend ($p<0.05$).

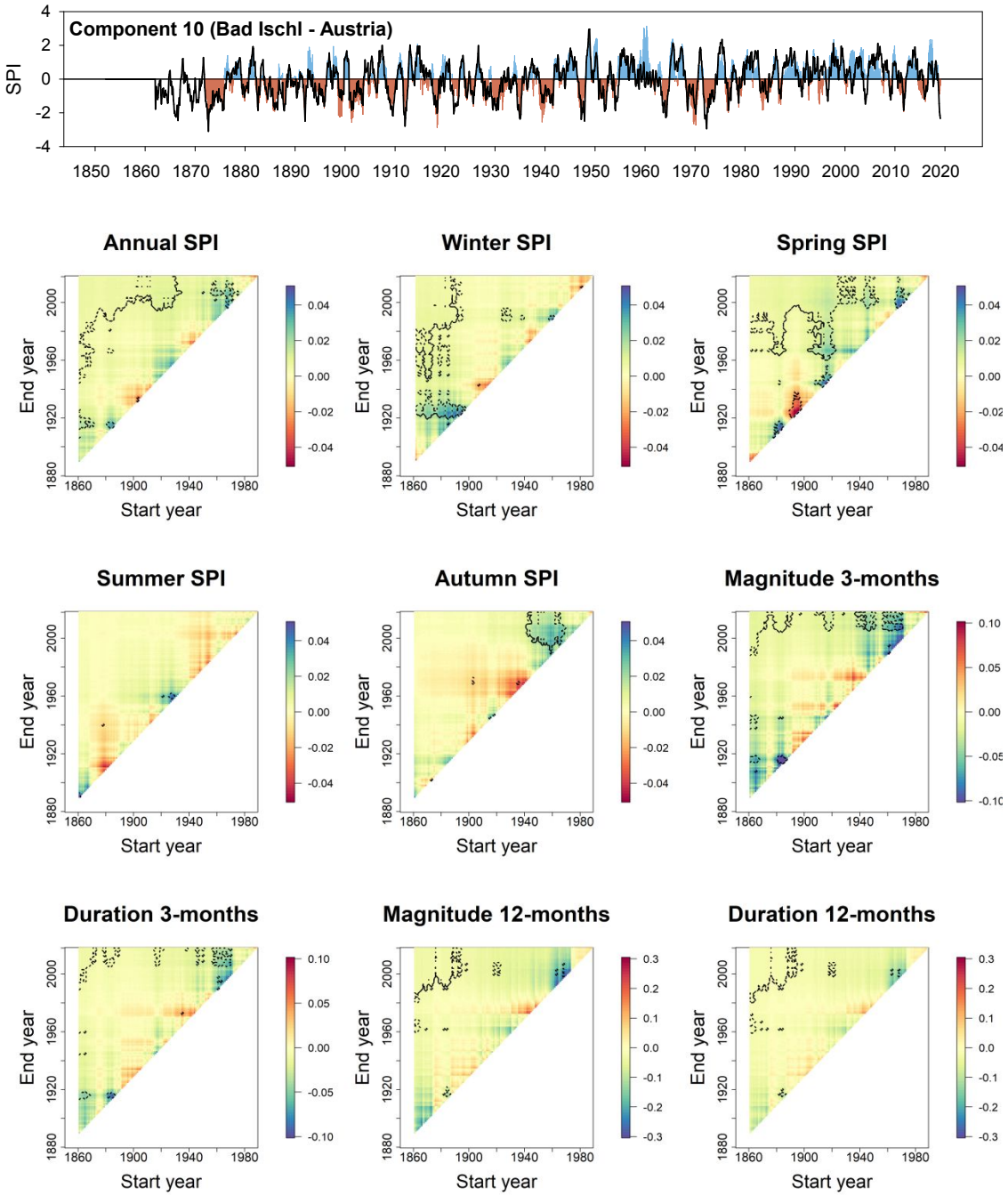

Supplementary Figure 9: Temporal evolution of the SPI-12 series of component 10 in color and the series of the most representative station (black line). The correlation between the series of the component and the series of the station is r = 0.78. Also shown are heat maps of 30-year running trends in annual and seasonal SPI and 3- and 12-month SPI drought duration and magnitude for the station of Badlschl (Austria). X and Y-axes indicate the start and end years, respectively, of the time slices for the running trend analysis. The scale indicates the magnitude of the trend based on the slope of the linear regression analysis. Dotted lines indicate periods with a significant trend ($p<0.05$).

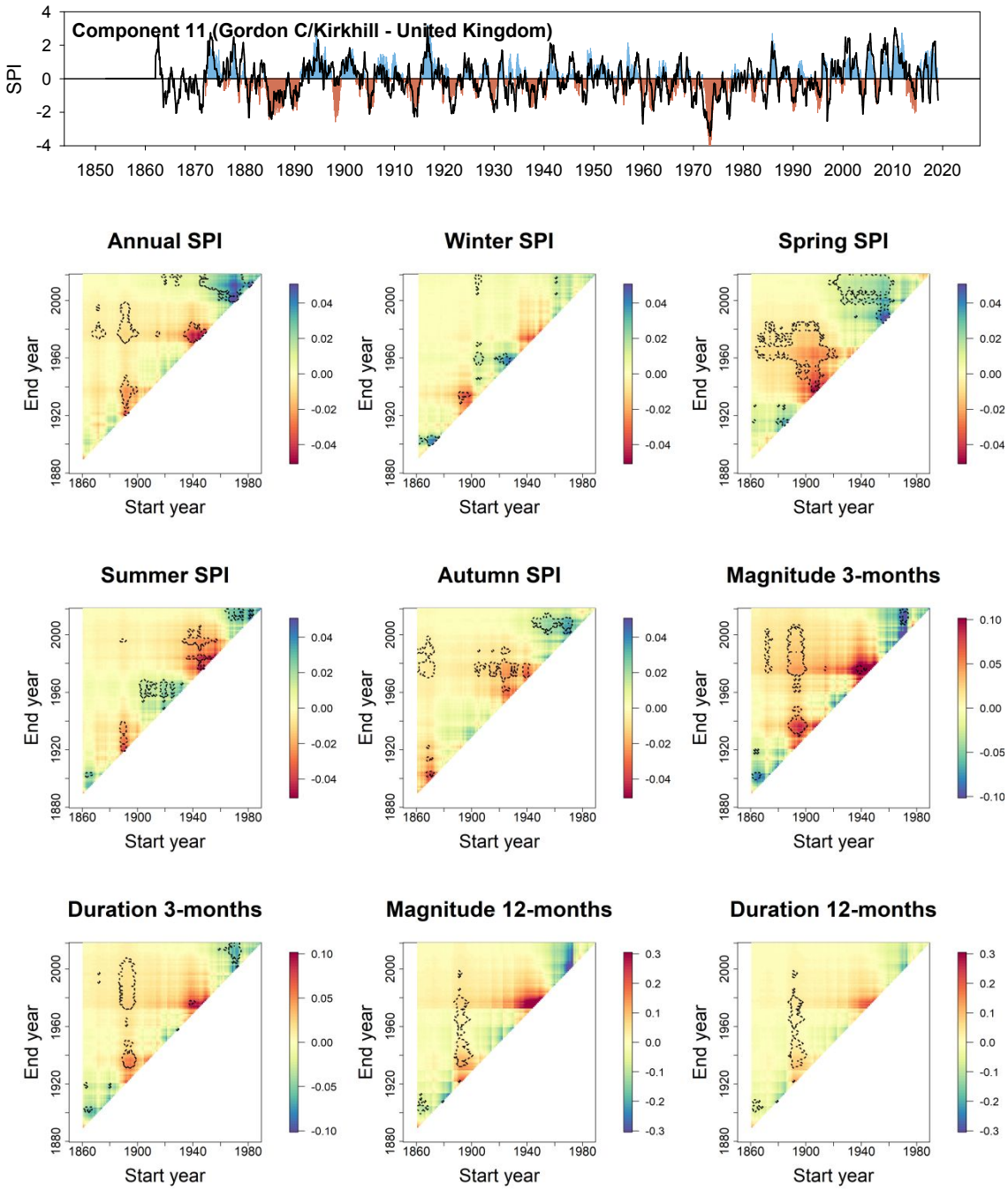

Supplementary Figure 10: Temporal evolution of the SPI-12 series of component 11 in color and the series of the most representative station (black line). The correlation between the series of the component and the series of the station is r = 0.75. Also shown are heat maps of 30-year running trends in annual and seasonal SPI and 3- and 12-month SPI drought duration and magnitude for the station of Gordoc C/Kirkhill (United Kingdom). X and Y-axes indicate the start and end years, respectively, of the time slices for the running trend analysis. The scale indicates the magnitude of the trend based on the slope of the linear regression analysis. Dotted lines indicate periods with a significant trend ($p<0.05$).

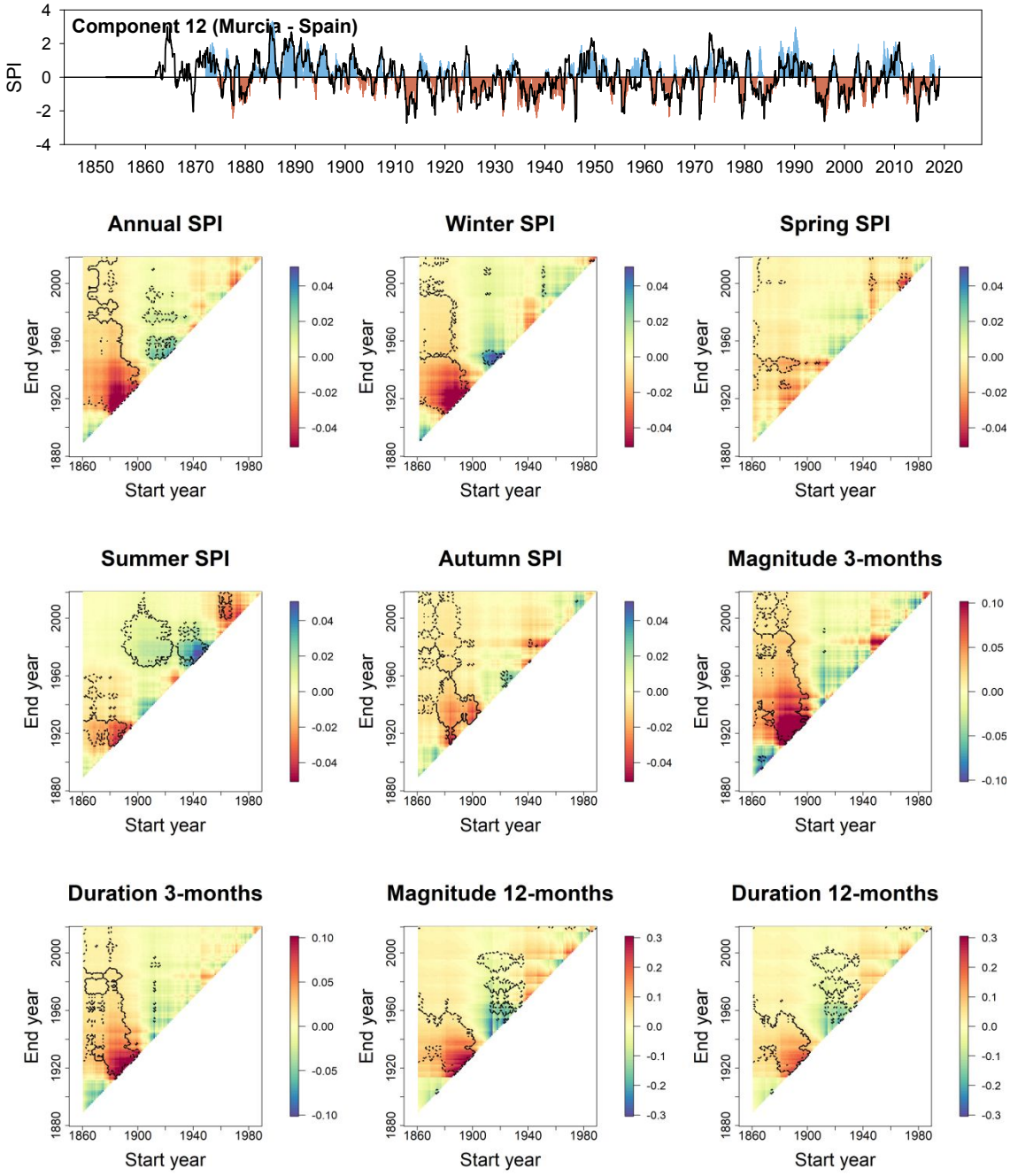

Supplementary Figure11: Temporal evolution of the SPI-12 series of component 12 in color and the series of the most representative station (black line). The correlation between the series of the component and the series of the station is r = 0.80. Also shown are heat maps of 30-year running trends in annual and seasonal SPI and 3- and 12-month SPI drought duration and magnitude for the station of Murcia (Spain). X and Y-axes indicate the start and end years, respectively, of the time slices for the running trend analysis. The scale indicates the magnitude of the trend based on the slope of the linear regression analysis. Dotted lines indicate periods with a significant trend ($p<0.05$).

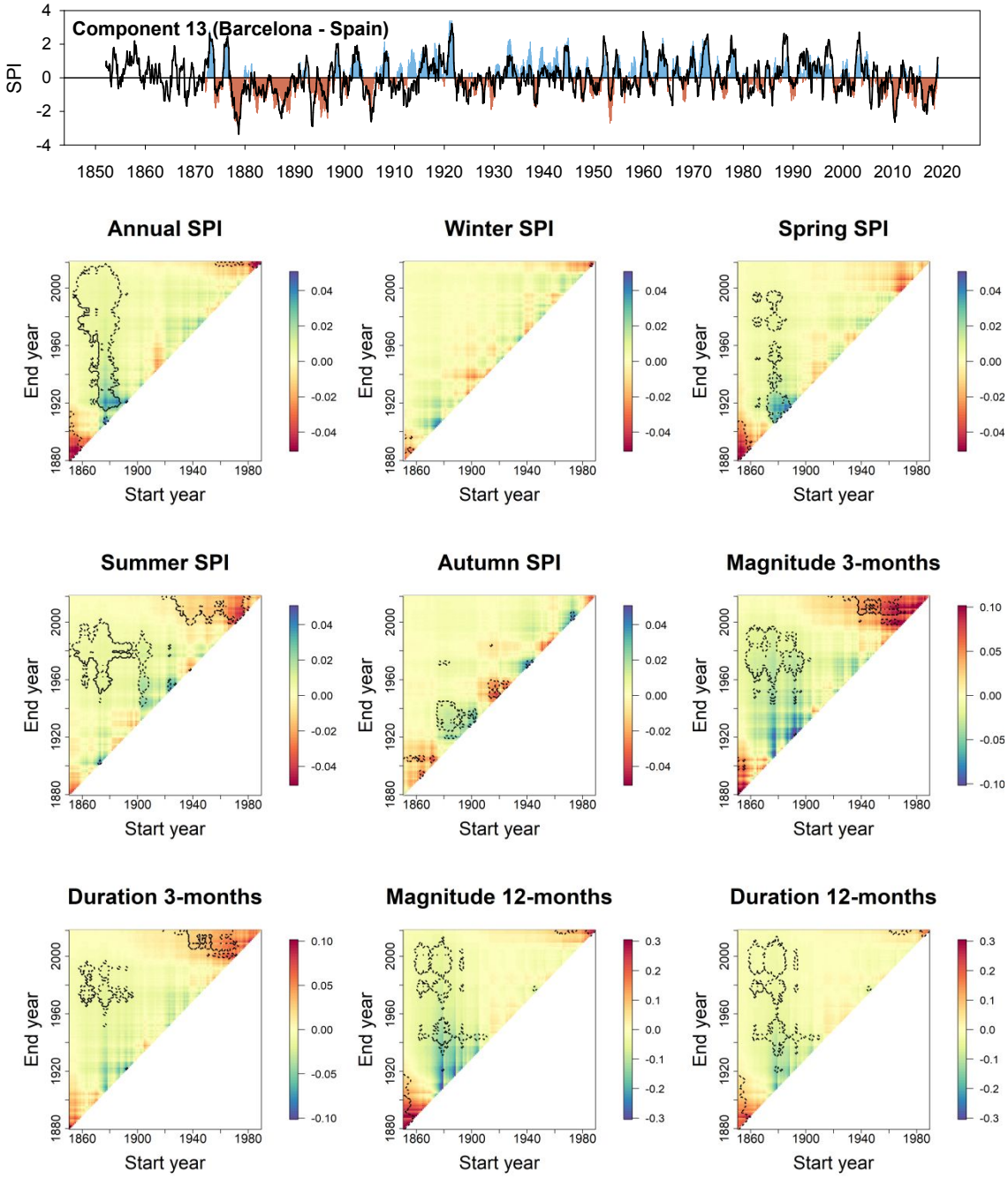

Supplementary Figure 12: Temporal evolution of the SPI-12 series of component 13 in color and the series of the most representative station (black line). The correlation between the series of the component and the series of the station is r = 0.76. Also shown are heat maps of 30-year running trends in annual and seasonal SPI and 3- and 12-month SPI drought duration and magnitude for the station of Barcelona (Spain). X and Y-axes indicate the start and end years, respectively, of the time slices for the running trend analysis. The scale indicates the magnitude of the trend based on the slope of the linear regression analysis. Dotted lines indicate periods with a significant trend ($p<0.05$).

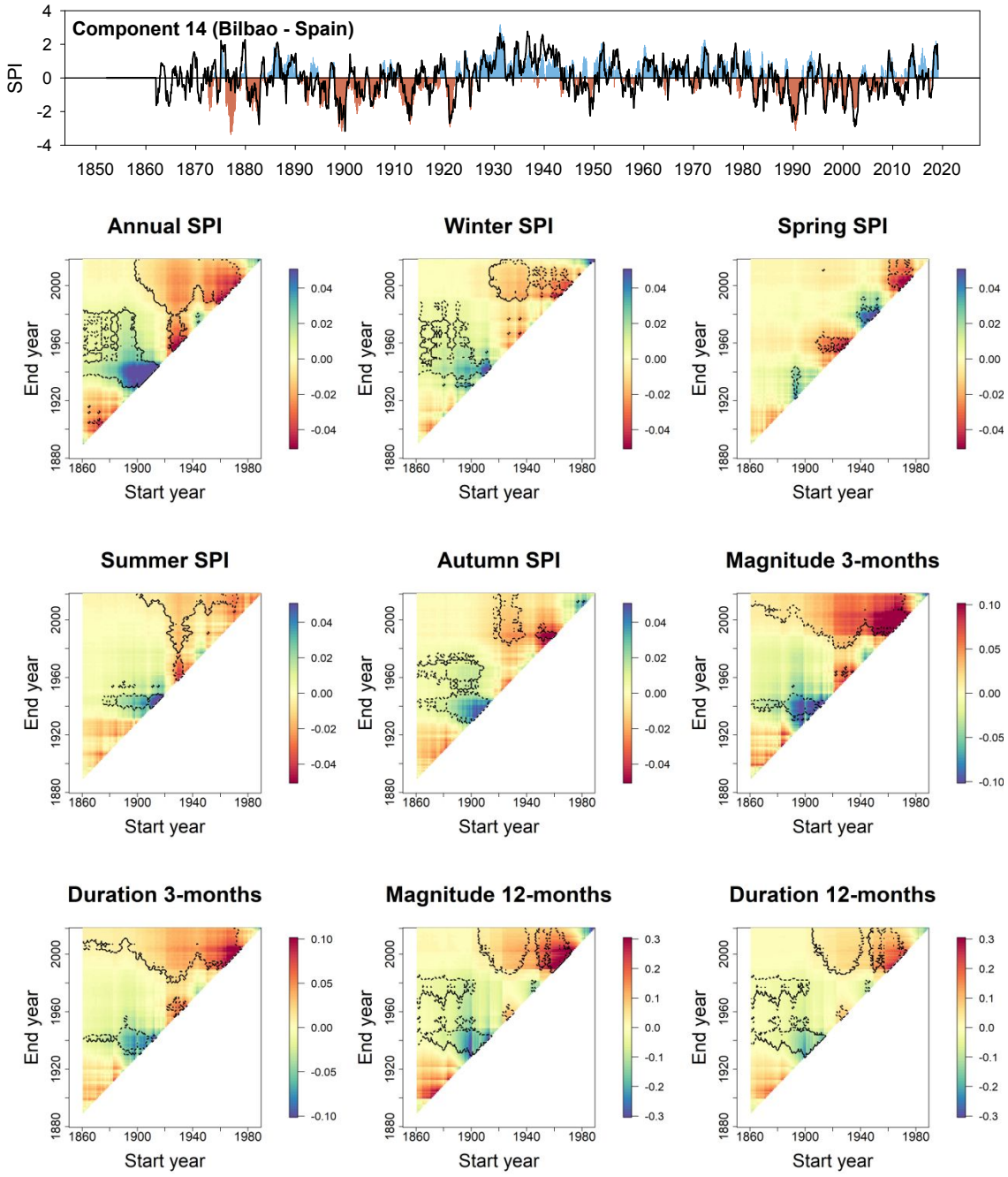

Supplementary Figure 13: Temporal evolution of the SPI-12 series of component 14 in color and the series of the most representative station (black line). The correlation between the series of the component and the series of the station is r = 0.75. Also shown are heat maps of 30-year running trends in annual and seasonal SPI and 3- and 12-month SPI drought duration and magnitude for the station of Bilbao (Spain). X and Y-axes indicate the start and end years, respectively, of the time slices for the running trend analysis. The scale indicates the magnitude of the trend based on the slope of the linear regression analysis. Dotted lines indicate periods with a significant trend ($p<0.05$).

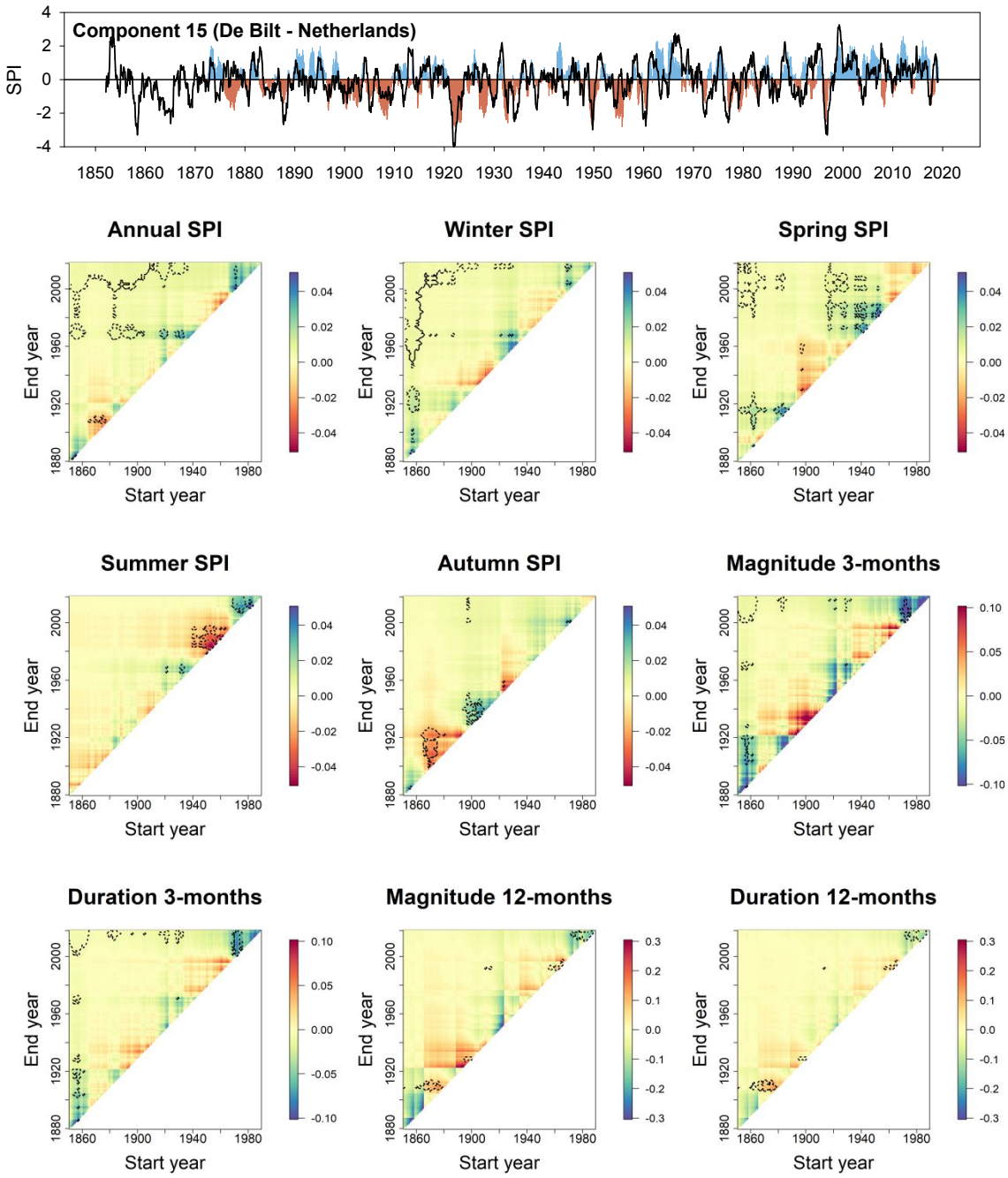

Supplementary Figure 14: Temporal evolution of the SPI-12 series of component 15 in color and the series of the most representative station (black line). The correlation between the series of the component and the series of the station is r = 0.51. Also shown are heat maps of 30-year running trends in annual and seasonal SPI and 3- and 12-month SPI drought duration and magnitude for the station of De Bilt (Netherlands). X and Y-axes indicate the start and end years, respectively, of the time slices for the running trend analysis. The scale indicates the magnitude of the trend based on the slope of the linear regression analysis. Dotted lines indicate periods with a significant trend ($p<0.05$).

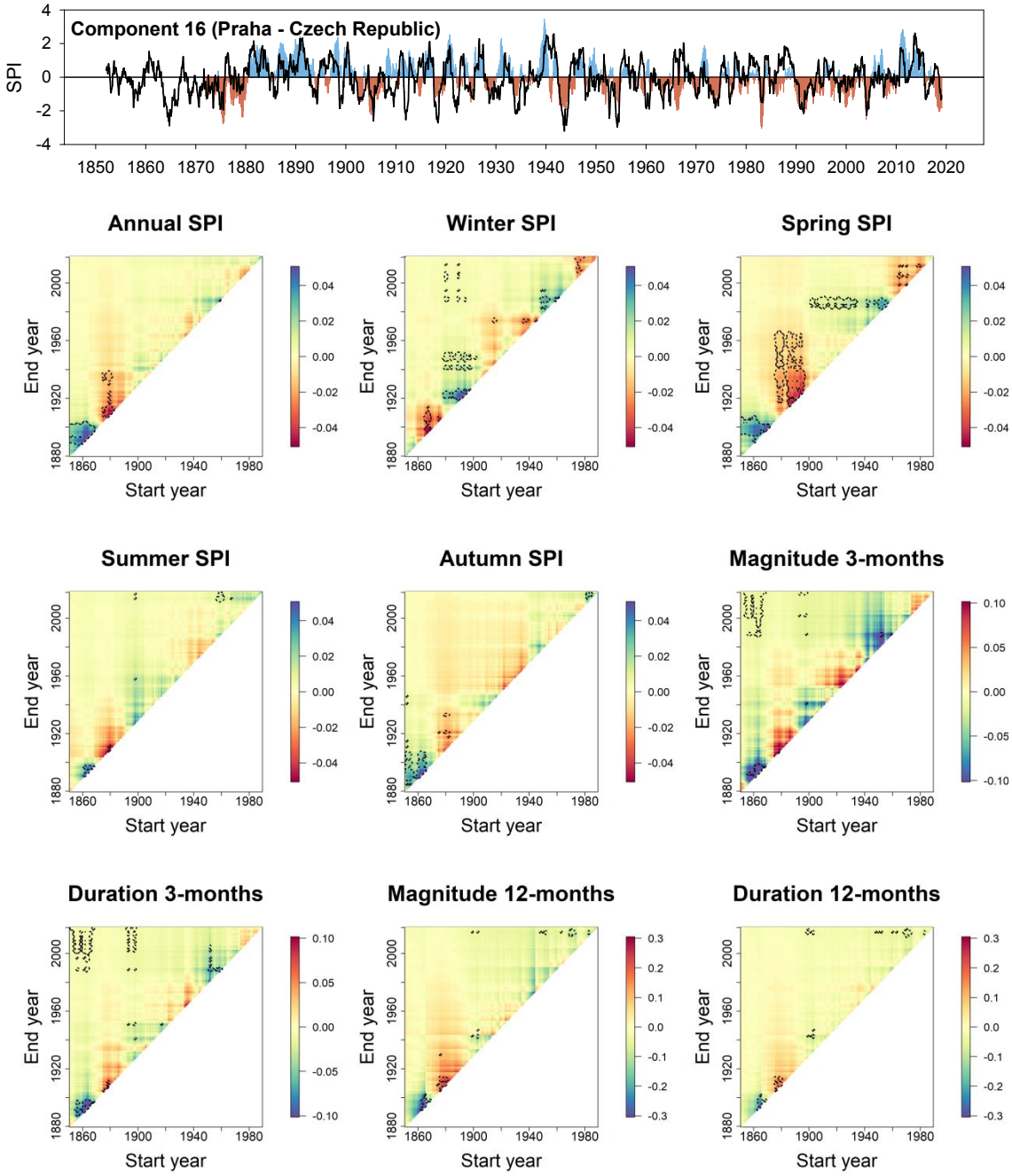

Supplementary Figure 15: Temporal evolution of the SPI-12 series of component 16 in color and the series of the most representative station (black line). The correlation between the series of the component and the series of the station is r = 0.52. Also shown are heat maps of 30-year running trends in annual and seasonal SPI and 3- and 12-month SPI drought duration and magnitude for the station of Praha (Czech Republic). X and Y-axes indicate the start and end years, respectively, of the time slices for the running trend analysis. The scale indicates the magnitude of the trend based on the slope of the linear regression analysis. Dotted lines indicate periods with a significant trend ($p<0.05$).

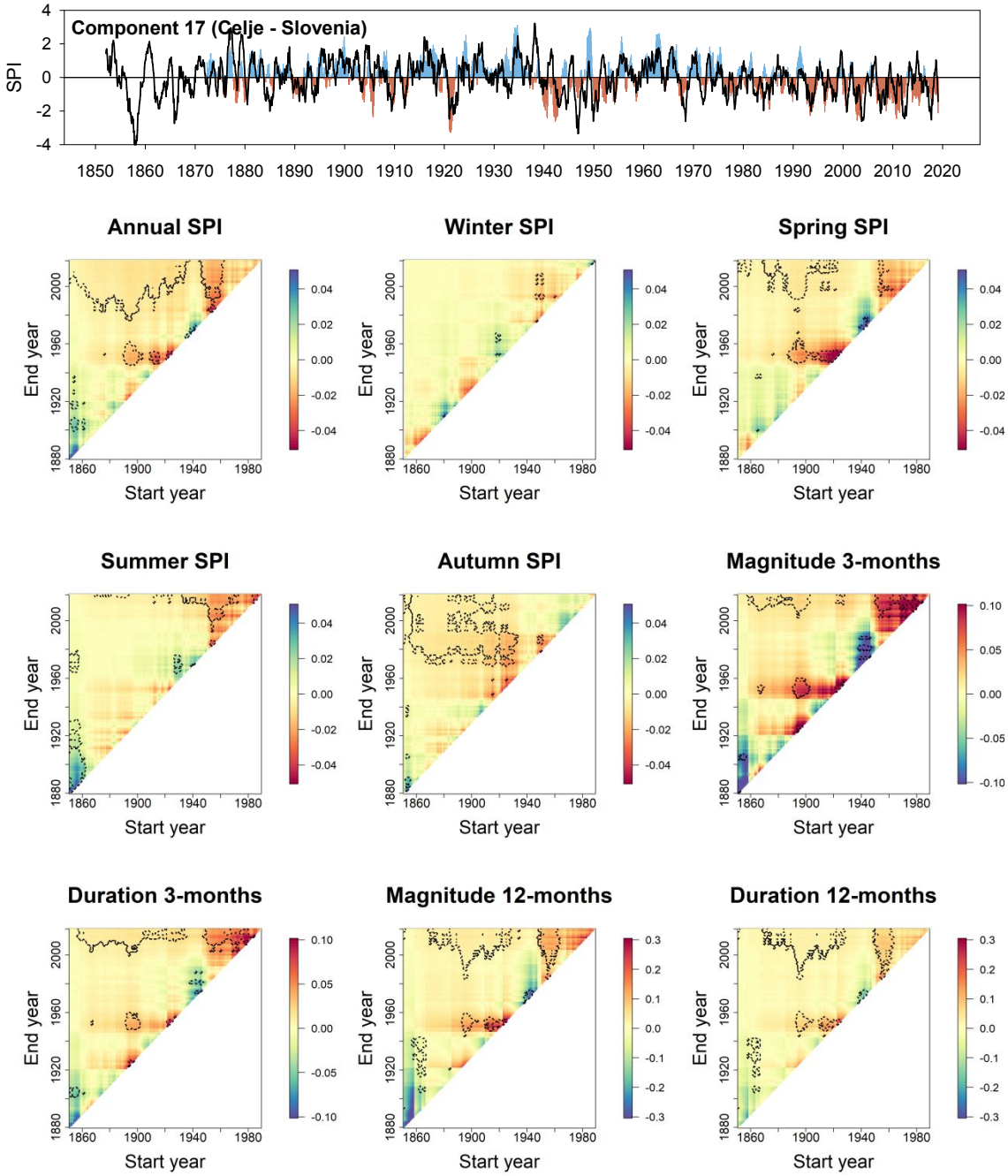

Supplementary Figure 16: Temporal evolution of the SPI-12 series of component 17 in color and the series of the most representative station (black line). The correlation between the series of the component and the series of the station is r = 0.54. Also shown are heat maps of 30-year running trends in annual and seasonal SPI and 3- and 12-month SPI drought duration and magnitude for the station of Celje (Slovenia). X and Y-axes indicate the start and end years, respectively, of the time slices for the running trend analysis. The scale indicates the magnitude of the trend based on the slope of the linear regression analysis. Dotted lines indicate periods with a significant trend ($p<0.05$).

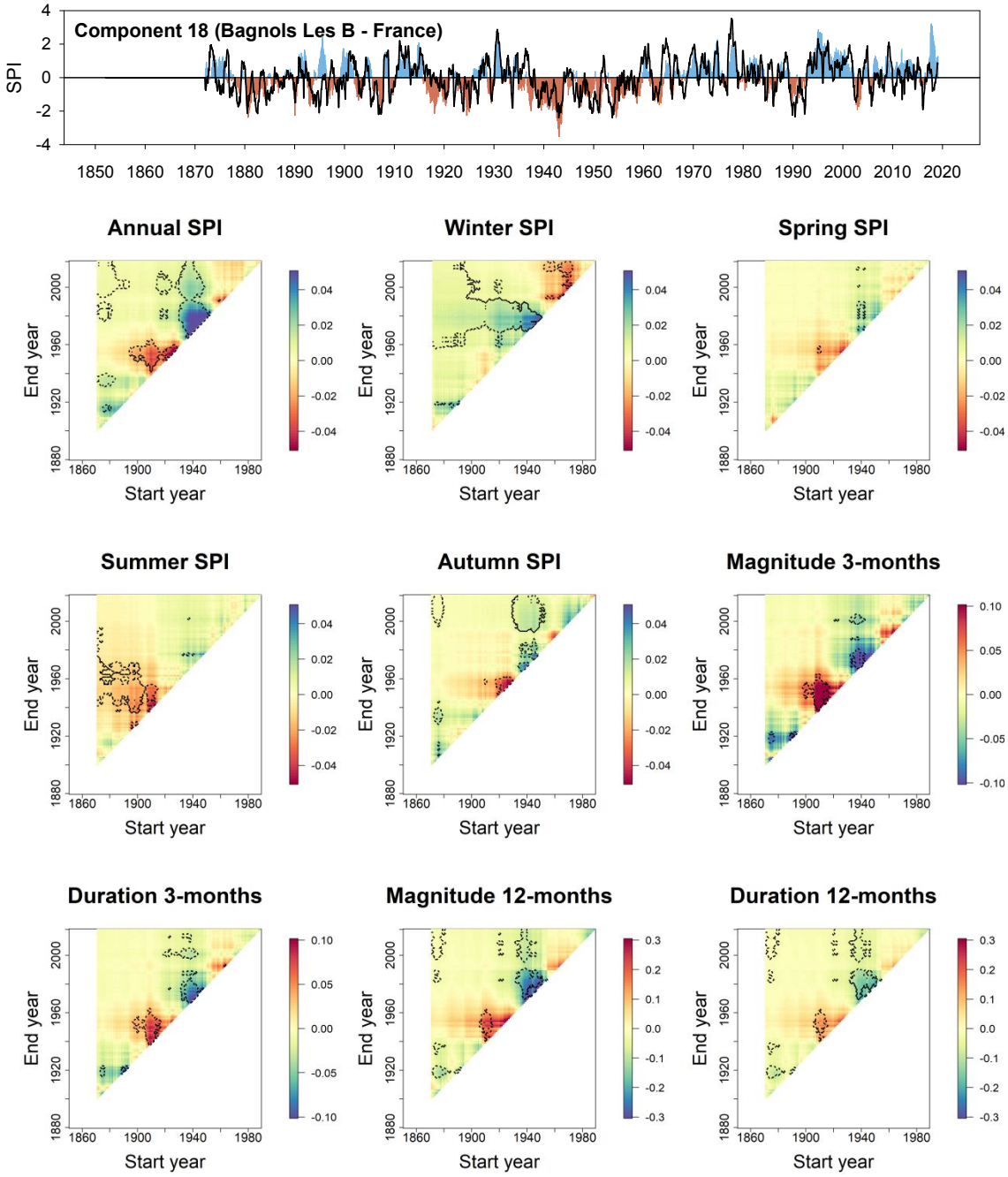

Supplementary Figure 17: Temporal evolution of the SPI-12 series of component 18 in color and the series of the most representative station (black line). The correlation between the series of the component and the series of the station is r = 0.60. Also shown are heat maps of 30-year running trends in annual and seasonal SPI and 3- and 12-month SPI drought duration and magnitude for the station of Bagnols les B (France). X and Y-axes indicate the start and end years, respectively, of the time slices for the running trend analysis. The scale indicates the magnitude of the trend based on the slope of the linear regression analysis. Dotted lines indicate periods with a significant trend ($p<0.05$).

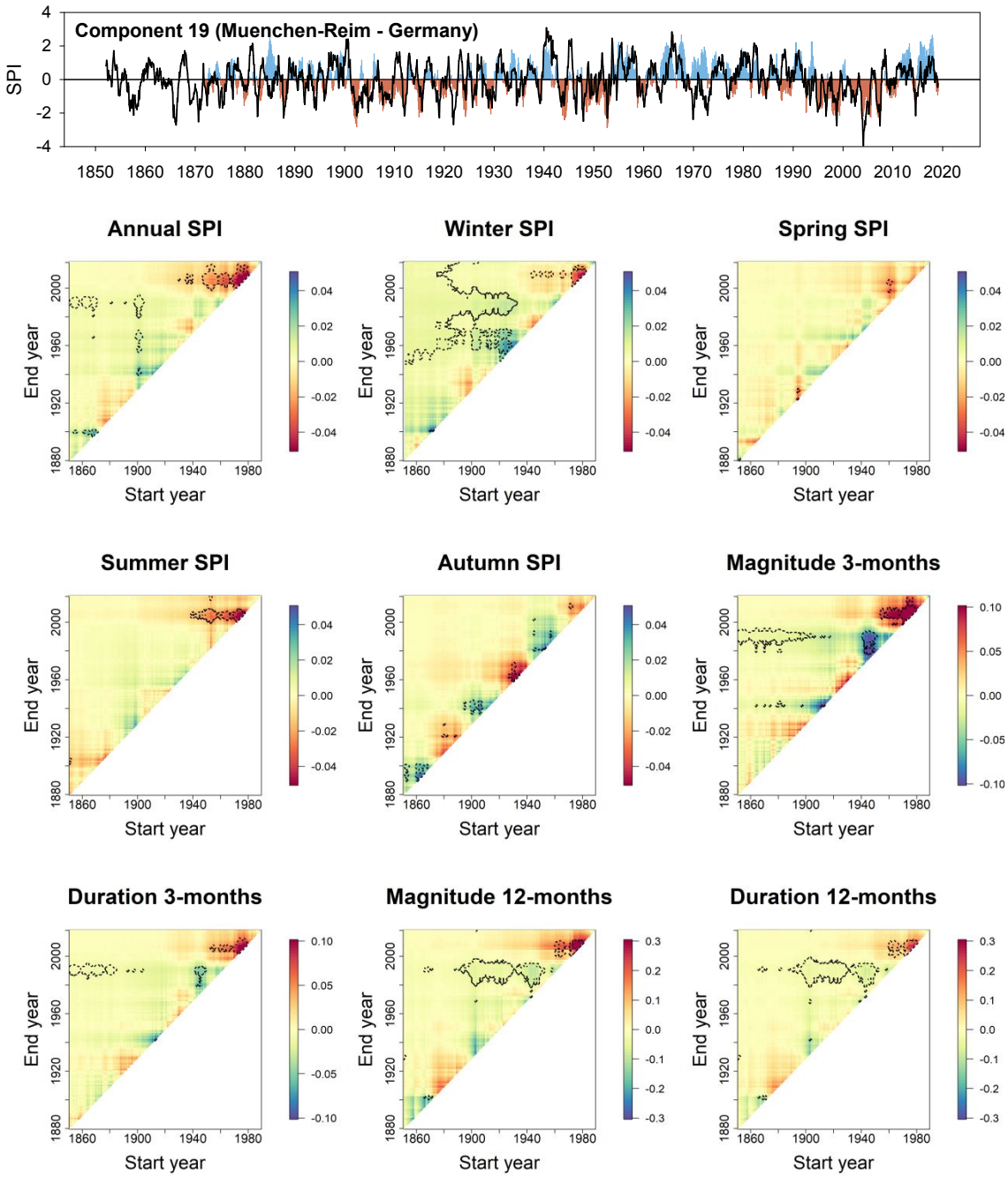

Supplementary Figure 18: Temporal evolution of the SPI-12 series of component 19 in color and the series of the most representative station (black line). The correlation between the series of the component and the series of the station is r = 0.50. Also shown are heat maps of 30-year running trends in annual and seasonal SPI and 3- and 12-month SPI drought duration and magnitude for the station of Muenchen-Reim (Germany). X and Y-axes indicate the start and end years, respectively, of the time slices for the running trend analysis. The scale indicates the magnitude of the trend based on the slope of the linear regression analysis. Dotted lines indicate periods with a significant trend ($p<0.05$).

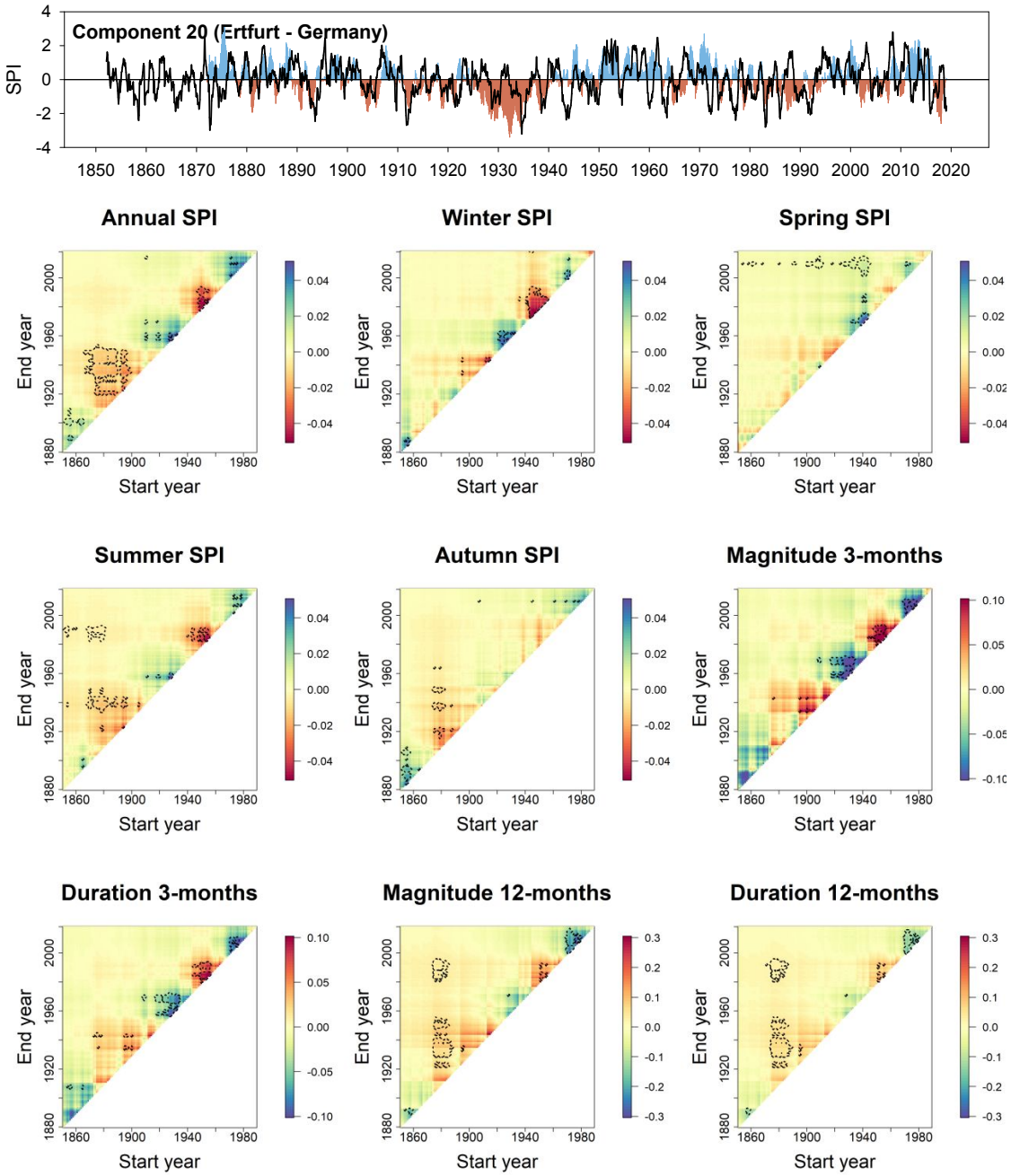

Supplementary Figure 19: Temporal evolution of the SPI-12 series of component 20 in color and the series of the most representative station (black line). The correlation between the series of the component and the series of the station is r = 0.28. Also shown are heat maps of 30-year running trends in annual and seasonal SPI and 3- and 12-month SPI drought duration and magnitude for the station of Ertfurt (Germany). X and Y-axes indicate the start and end years, respectively, of the time slices for the running trend analysis. The scale indicates the magnitude of the trend based on the slope of the linear regression analysis. Dotted lines indicate periods with a significant trend ($p<0.05$).

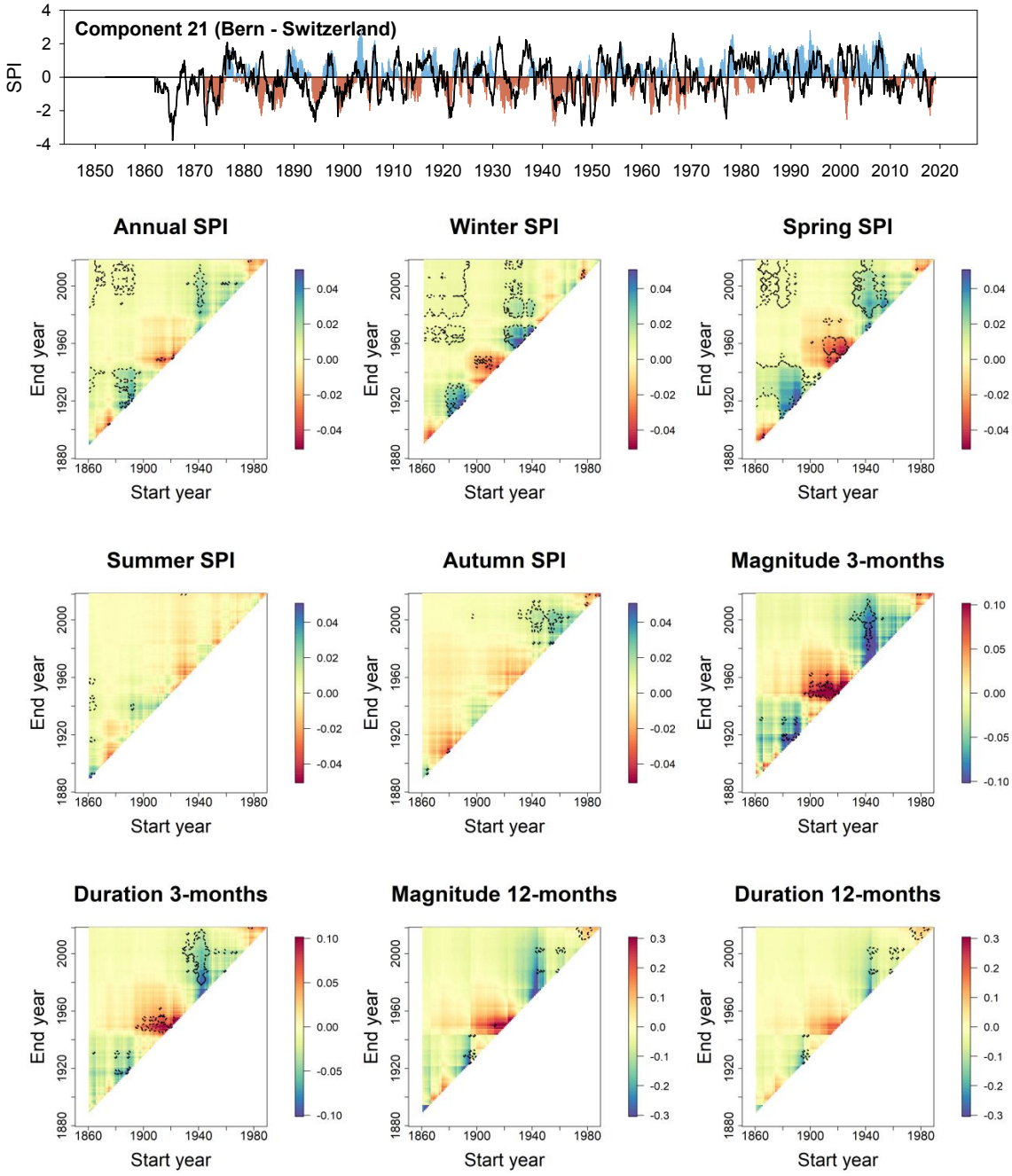

Supplementary Figure 20: Temporal evolution of the SPI-12 series of component 21 in color and the series of the most representative station (black line). The correlation between the series of the component and the series of the station is r = 0.32. Also shown are heat maps of 30-year running trends in annual and seasonal SPI and 3- and 12-month SPI drought duration and magnitude for the station of Bern (Switzerland). X and Y-axes indicate the start and end years, respectively, of the time slices for the running trend analysis. The scale indicates the magnitude of the trend based on the slope of the linear regression analysis. Dotted lines indicate periods with a significant trend ($p<0.05$).

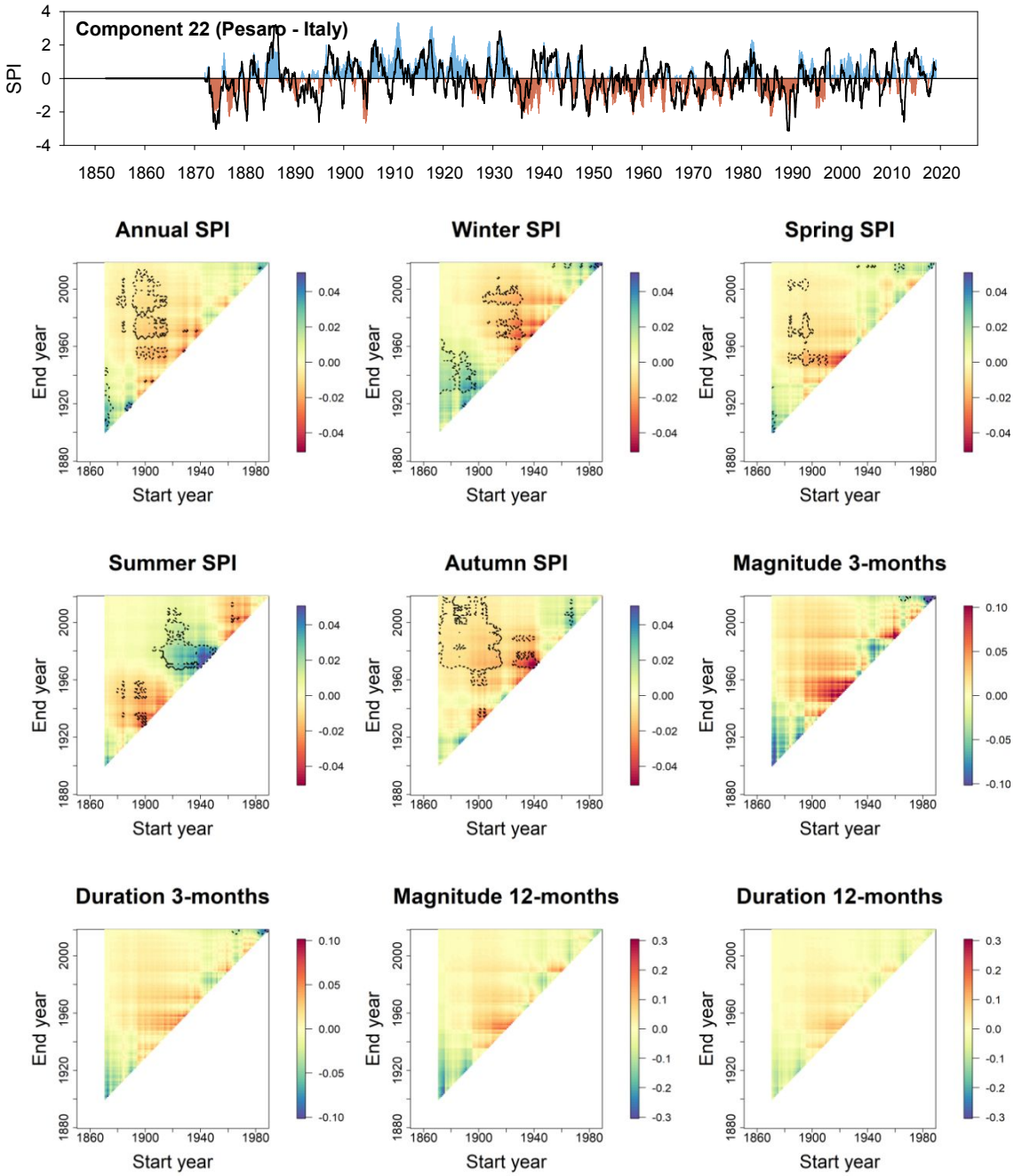

Supplementary Figure 21: Temporal evolution of the SPI-12 series of component 22 in color and the series of the most representative station (black line). The correlation between the series of the component and the series of the station is r = 0.54. Also shown are heat maps of 30-year running trends in annual and seasonal SPI and 3- and 12-month SPI drought duration and magnitude for the station of Pesano (Italy). X and Y-axes indicate the start and end years, respectively, of the time slices for the running trend analysis. The scale indicates the magnitude of the trend based on the slope of the linear regression analysis. Dotted lines indicate periods with a significant trend ($p<0.05$).

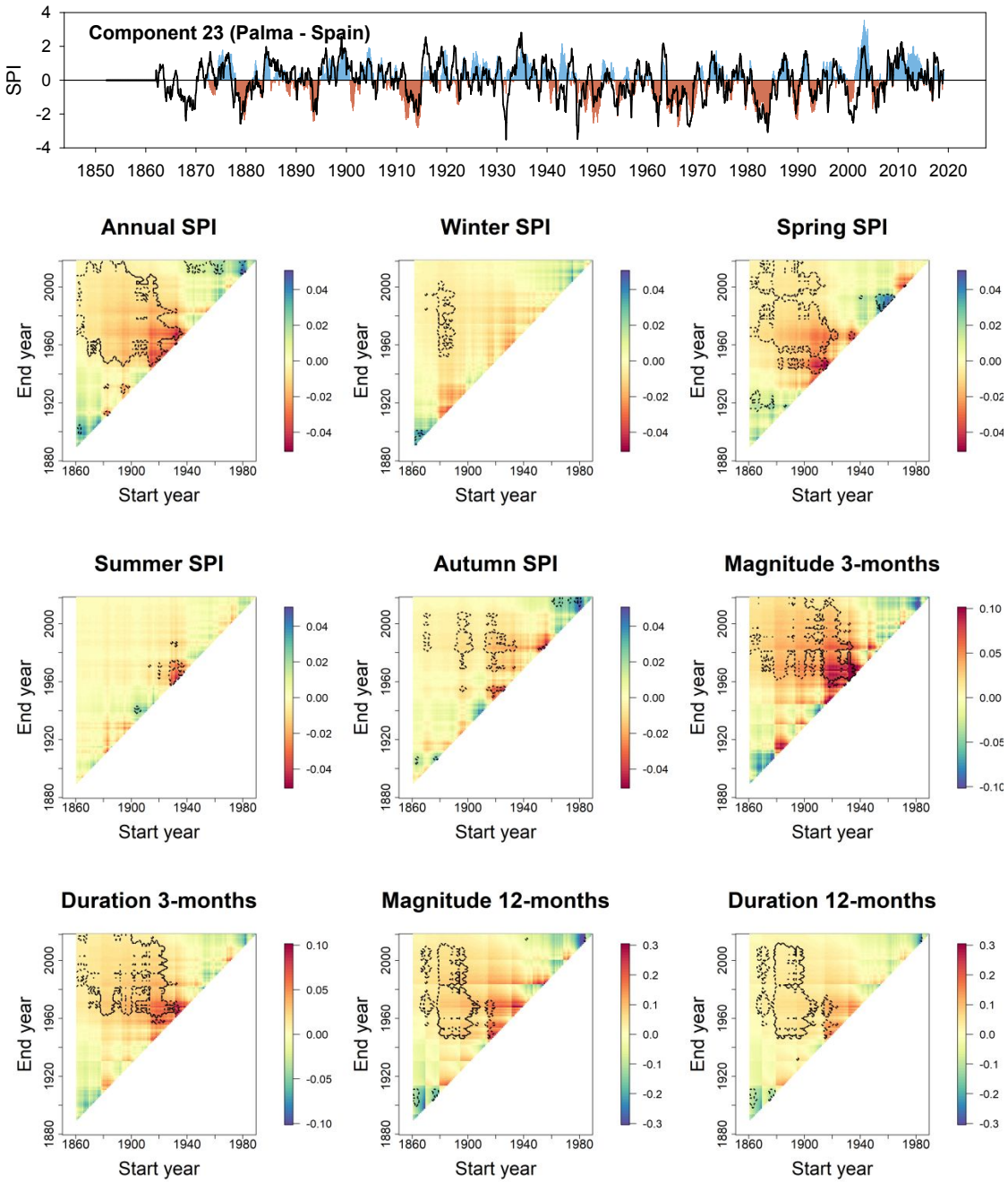

Supplementary Figure 22: Temporal evolution of the SPI-12 series of component 23 in color and the series of the most representative station (black line). The correlation between the series of the component and the series of the station is r = 0.64. Also shown are heat maps of 30-year running trends in annual and seasonal SPI and 3- and 12-month SPI drought duration and magnitude for the station of Palma (Spain). X and Y-axes indicate the start and end years, respectively, of the time slices for the running trend analysis. The scale indicates the magnitude of the trend based on the slope of the linear regression analysis. Dotted lines indicate periods with a significant trend ($p<0.05$).